Final Report

January 1998

Environmental Studies Relative to Potential Sand Mining in the Vicinity of the City of Virginia Beach, Virginia

Part 3: Nearshore Waves and Currents Observations and Modeling

Author:

John D. Boon
Virginia Institute of Marine Science

Project Manager:

Carl H. Hobbs, III
Virginia Institute of Marine Science

Prepared under MMS Cooperative Agreement 14-35-0001-3087 through Virginia Institute of Marine Science of the College of William & Mary

MMS U.S. Department of the Interior
Minerals Management Service

College of William and Mary
Virginia Institute of Marine Science
School of Marine Science

DISCLAIMER

This report has been reviewed by the Minerals Management Service and approved for publication. Approval does not signify that the contents necessarily reflect the views and policies of the Service, nor does mention of trade names or commercial products constitute endorsement or recommendation for use.

The Department of the Interior

As the Nations's principal conservation agency, the Department of the Interior has responsibility for most of our nationally owned public lands and natural resources. This includes fostering sound use of our land and water resources, protecting our fish, wildlife, and biological diversity, preserving the environmental and cultural values of our national parks and historic places; and providing for the enjoyment of life through outdoor recreation. The Department assesses our energy and mineral resources and works to ensure that their development is in the best interests of all our people by encouraging stewardship and citizen participation in their care. The Department also has a major responsibility for American Indian reservation communities and for people who live in island territories under U.S. Administration.

The Minerals Management Service Mission

As a bureau of the Department of the Interior, the Minerals Management Service's (MMS) primary responsibilities are to manage the mineral resources located on the Nations's Outer Continental Shelf (OCS), collect revenue from the Federal OCS and onshore federal and Indian lands, and distribute those revenues.

Moreover, in working to meet its responsibilities, the Offshore Minerals Management Program administers the OCS competitive leasing program and oversees the safe and environmentally sound exploration and production of our Nation's offshore natural gas, oil and other mineral resources. The MMS Royalty Management Program meets its responsibilities by entrusting the efficient, timely and accurate collection and distribution of revenue from mineral leasing and production due to Indian tribes andallottees, States and the U. S. Treasury

the MMS strives to fulfill its responsibilities through the general guiding principles of: (1) being responsive to the public's concerns and interests by maintaining a dialog with all potentially affected parties and (2) carrying out its programs with an emphasis on working to enhance the quality of life for all Americans by lending MMS assistance and expertise to economic development and environmental protection.

Environmental Studies Relative to Potential Sand Mining in the Vicinity of the City of Virginia Beach, Virginia

Nearshore Waves and Currents – Observations and Modeling

Introduction

This report will address nearshore wave modeling results for the City of Virginia Beach and the beach community of Sandbridge, Virginia. Wave and near-bottom current observations made near the Chesapeake Bay entrance will not be presented here in order to focus attention on wave modeling results for a now active sand mining site located approximately 5 km (2.7 nm) due east of Sandbridge. A nested-grid, spectral wave propagation model was applied to investigate the potential change in maximum wave heights expected for the nearshore region between that site and the surf zone at Sandbridge. The purpose of this report is to describe the model and its application to the Virginia Beach – Sandbridge coastal sector, and to provide an analysis of the results obtained.

Sand Mining Borrow Areas

Detailed site information was recently received for two adjacent borrow areas located on a nearshore ridge formation known as Sandbridge Shoal (Fig. 1). One of these areas, designated borrow site "A" by Federal authorities, was dredged in mid-1996 to yield approximately 810,000 cubic yards (619,289 cu. m.) of beach nourishment material for the U.S. Navy's Fleet Combat Training Center at Dam Neck, Virginia. At the time of writing of this report, it was anticipated that an additional 1.3 million cubic yards (994,000 cu. m.) of material would be extracted from borrow area "A" or a closely located second site to the north designated borrow site "B". This material will be used for restoration of Sandbridge Beach to the south of Dam Neck. Approximately 500,000 cubic yards (383,000 cu. m.) of material is to be removed at two year intervals in the future. Borrow area "A" has an irregular plan-view area of approximately 2.4 million square meters and borrow area "B" occupies an area of about 2.1 million square meters.

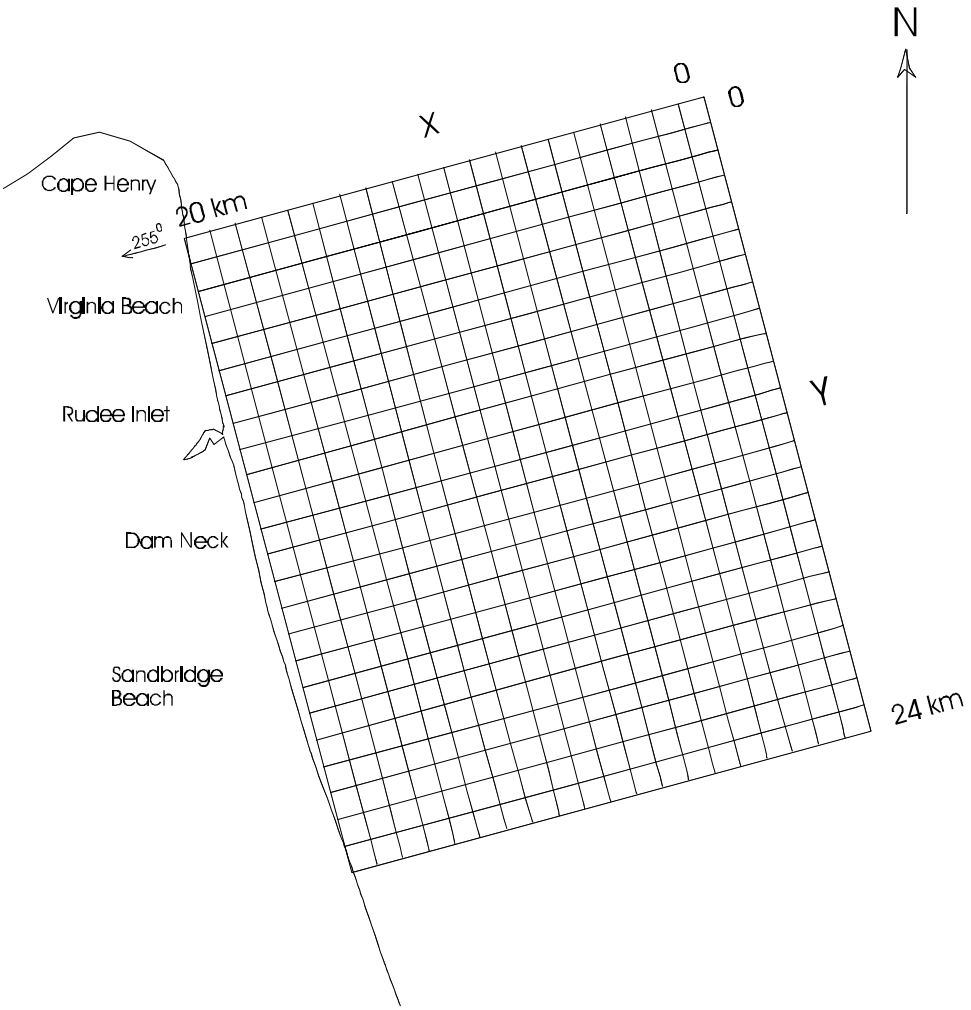

Figure 1. Map showing location of Virginia Beach – Sandbridge reference grid

Wave Model Description

The wave model selected for use in this study is the University of Delaware's combined refraction/diffraction model for spectral wave conditions, REF/DIF S (Kirby and Ozkan, 1992). It differs from its monochromatic wave predecessor, REF/DIF 1 (Dalrymple and Kirby, 1991), in that it simulates the behavior of a random sea through use of a two-dimensional wave spectrum

in which the wave energy density is a function of both frequency and direction. Water surface elevation at any point in the model domain is thus represented by a series of component waves,

$$h = \sum_{f} \sum_{q} A(f,q) e^{iy} \qquad (1)$$

where *A(f,2)* is the complex amplitude for a wave of frequency f and direction *2*, and

$$y = \int \vec{k} \cdot d\vec{x} - wt + f \qquad (2)$$

is its phase given

$$\vec{k} = \vec{i}k_x + \vec{j}k_y = 2p\vec{i} / L_x + 2p\vec{j} / L_y$$

as the wave number vector defined by its components (wavelengths) in the x and y directions, $T = 2\pi f$ as the radian frequency, and ϕ as a random phase component.

For input, REF/DIF S requires a two-dimensional wave spectrum specified by a matrix of discrete, band-centered values of frequency and direction. The separate wave components represented by the elements in this matrix are propagated simultaneously through a model grid, permitting a statistical representation of the local wave height at each intersection in the grid. Although the model does not account for interaction between wave components, it is weakly nonlinear and permits efficient calculation of a wave height parameter employing an adequate sample size. For example, a spectrum represented by 11 directions for each of 11 frequency bands would yield a total of n=121 discrete wave components propagated simultaneously. REF/DIF S calculates the significant wave height as

$$H_s = \left[8 \sum_{p=1}^{n} \left| A_p \right|^2 \right]^{1/2} \qquad (3)$$

where $\boldsymbol{A_p}$ is the complex amplitude of the *p*th component wave at a given grid location. In most applications, the significant wave height, H_s, and the zero-moment wave height, Hm_o, are considered equivalent. H_s ,or $H_{1/3}$, is defined as the average height of the highest one-third of the waves in a sample record. Hm_o is defined on the basis of the total wave energy, m_0, as

$$Hm_0 = 4\sqrt{m_0} \qquad (4)$$

with m_0 computed as the variance of the surface elevation. Wave heights throughout this report will be referred to as the zero-moment wave height, $Hm_o \approx H_s$.

REF/DIF 1 and REF/DIF S are both parabolic wave models based on the mild slope equation

$$\nabla_h \cdot (CC_g \nabla_h h) + k^2 CC_g h \qquad (6)$$

with $C = \sqrt{(g/k)\tanh kh}$ as the wave celerity and $C_g = C(1 + 2kh/\sinh 2kh)/2$ as the wave group velocity, and g = acceleration of gravity. A linear approximation to eq. (6),

$$\frac{\partial A}{\partial x} = \frac{i}{2k}\frac{\partial^2 A}{\partial y^2} - \frac{w}{2C_g}A - \alpha A \qquad (7)$$

is used to simulate waves traveling over irregular bottom topography and includes the effects of shoaling, refraction, energy dissipation (*w* is an energy dissipation factor), wave breaking (α is a breaking coefficient) and diffraction (Kirby, 1986; Kirby and Dalrymple, 1986). A restriction of the present REF/DIF models is that waves must propagate within approximately 50^0 of the principal wave direction that is usually aligned with the downwave or positive x-axis of the model grid. The user must specify a constant complex amplitude, $A(f,\theta)$, for each f,θ pair along the y-axis of the starting row. Dalrymple and Kirby (1991) list the following additional assumptions and features of REF/DIF S:

Mild Bottom Slope. Model equations are based on the assumption that variations in depth occur over distances that are long in comparison to a wavelength. Solutions are considered accurate for bottom slopes up to 1:3 and to show the correct trends in wave height over steeper slopes.

Weak nonlinearity. The model is based on a Stokes perturbation expansion and is therefore restricted to deep-water applications where Stokes waves are valid. Nonlinearity is measured by

the Ursell parameter $U=HL^2/h^3$. When U>40, Stokes waves are considered invalid and a "patch" to a solitary wave is used that is considered valid in shallow water. To achieve this, REF/DIF S uses a hybrid model with a modified dispersion relationship for shallow water incorporating H_s calculated for each grid row proceeding in the landward direction

$$s^2 = gk \tanh(kh(1 + H_s / 2h)) \qquad (8)$$

Turbulent bottom boundary layer. Three options for wave energy dissipation are available in REF/DIF S. The option used in the present study was that of a turbulent bottom boundary layer represented by a constant value of the Darcy-Weisbach friction factor, f_w = 0.01, in the dissipation factor,

$$w = \frac{2s\,kf_w|A|}{3p\,\sinh 2kh \sinh kh} \qquad (9)$$

It should be noted that f_w can be expected to vary as a function of the bed roughness so that it is likely to vary from point to point in the bottom grid.

Wave breaking. The breaking model used in REF/DIF S is that of Thornton and Guza (1983). The decay of the wave height is obtained from the energy dissipation for breaking waves (bore dissipation) given by

$$\frac{\partial EC_g}{\partial x} = -e_b \qquad (10)$$

where $E = \frac{1}{8}\rho g H_{rms}^2$ and $e_b = \frac{3\sqrt{\pi}}{16}\frac{\rho g f_p B^3}{\gamma^4 h^5} H_{rms}^7$

In the above, f_p is the spectral peak frequency, $H_s=1.414H_{rms}$, and B, γ are constants (B=1 and γ=0.6). The breaking coefficient α, as used in eq. (7), is very small for nonbreaking waves but, computed as

$$a = \frac{4e_b}{\rho g H_{rms}^2} \qquad (11)$$

becomes large as breaking conditions are reached and wave height reduces accordingly.

Subgrids. One of the most useful features of REF/DIF S is the subgrid option. After the user has first constructed a coarse-scale, rectangular **reference grid** of position and depth values defining the model domain, a rectangular **subgrid** may be set up defining a fine-scale sub-region of that domain. One can choose a grid cell-size for the subgrid that is many times smaller than that used for the reference grid. This allows local representation of key benthic features (e.g., artificial mounds or depressions) on a spatial scale of tens of meters while the remainder of the domain is represented at scales of hundreds of meters or kilometers.

Reference grid - subgrid combinations are particularly advantageous when used with spectral wave models because spectral wave information (measured or simulated) is usually available (and spatially uniform) only at offshore sites in deep water and not in the shallow nearshore region where the interaction of waves with bottom topography is frequently the study object. Spectral models propagate a combination of waves of different frequency and direction through the transition region from deep to shallow water. Because these component waves respond differently to dynamic processes (shoaling, refraction, diffraction, breaking) along the way, predicting the final sum of their heights at each grid intersection is anything but trivial. Local wave height extremes (high or low) may result from a combination of superposed waves travelling the same or different routes. This depends not only on the topography en route but also

on spectrum widths (broad or narrow) and selective wave breaking. Clearly, these same extremes could not be reproduced using a monochromatic wave model.

Other features and some restrictions. In addition to the features just described, REF/DIF S can model wave-current interaction. To use this option, the user must include horizontal (u,v) current components at reference grid (subgrid) intersections along with depth. The user may also choose an option that computes radiation stress components S_{xx}, S_{xy}, and S_{yy} at each intersection and writes them to an output file. While these features are available within the model domain, there is no interaction between propagating wave components nor is there any provision for momentum

transfer to any of these components from the atmosphere through specification of a surface wind field.

Spectral Input – the TMA Spectrum and Mitsuyasu-type Spreading Function

To provide input to REF/DIF S, a directional wave spectrum is required representing the distribution of wave energy in the frequency domain and in direction (angle θ). The relationship is expressed as

$$S(f,q) = S(f)G(f;q) \tag{12}$$

where $G(f;\theta)$ is the directional spreading function given by Mitsuyasu et al. (1975) as

$$G(f:q) = G_0 \cos^{2s}\left(q/2\right) \tag{13}$$

where θ is the direction angle measured counterclockwise from the principal wave direction or mean direction of wave advance (θ_m) and *s* is a parameter related to the frequency. If $\theta_{min} = -\pi$ and $\theta_{max} = \pi$, the constant G_0 becomes

$$G_0 = \frac{1}{p} 2^{2s-1} \frac{\Gamma^2(s+1)}{\Gamma(2s+1)} \tag{14}$$

where Γ is the Gamma function. The parameter *s* represents the degree of directional energy concentration and reaches a peak value, s_{max}, near the peak frequency, f_p. Goda and Suzuki (*in* Goda, 1985), introduced s_{max} as an engineering parameter in the expression

$$s = s_{max}(f / f_p)^5 \text{ when } f \le f_p; \text{ otherwise, } s = s_{max}(f / f_p)^{-2.5}$$

Goda (1985) considered s_{max} = 10 to be typical of local wind waves with s_{max} = 25 representing swell with a short decay distance and relatively large wave steepness. Figure 2 shows an example of the Mitsuyasu-type spreading function.

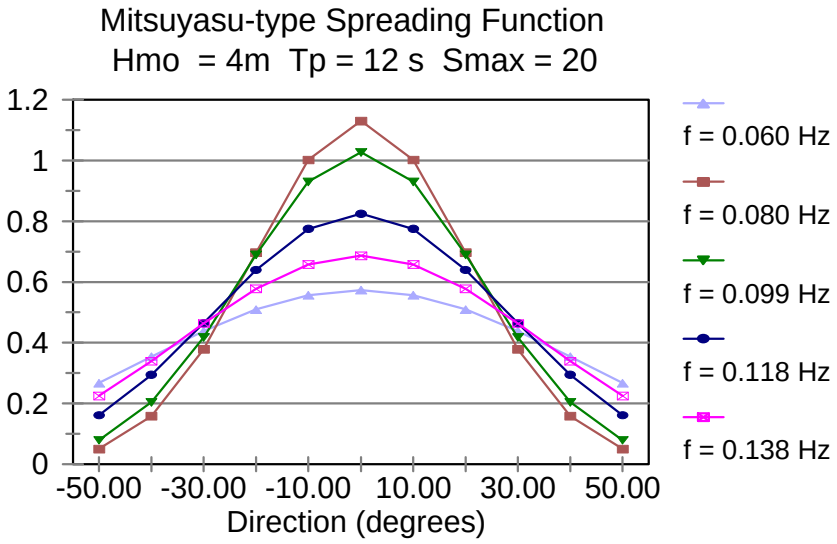

Figure 2. Mitsuyasu-type spreading function varying as a function of frequency.

Considering the frequency distribution in eq. 12, one may use experimentally derived formulations such as the JONSWAP spectrum, $S_J(f)$, (Hasselmann et al., 1973) for deep water or the TMA spectrum, $S_{TMA}(f,h)$, (Bouws et al., 1985) for finite depths. The JONSWAP spectrum and the TMA spectrum differ by $\phi_K(\omega_h)$, a transformation factor (Kitaigorodskii et al.,1975) in

$$S_{TMA}(f,h) = S_J(f) f_K(w_h) \qquad (15)$$

where $\omega_h = 2\pi f(h/g)^{1/2}$ is the dimensionless radian frequency, h = depth, g = acceleration due to gravity. In deep water ($\omega_h > 2$) ϕ_K is equal to unity and the two spectral forms in eq.(15) are equivalent. However, in shallow ($\omega_h < 1$) and intermediate ($1 \le \omega_h \le 2$) depths, they differ by ϕ_K =

$0.5\omega_h^2$ and $\phi_K = 1 - 0.5(2-\omega_h)^2$, respectively [Hughes, 1984]. The JONSWAP spectrum itself may be computed in terms of wave height, frequency, and a spectrum "peakedness" parameter, λ, as

$$S_f(f) = \frac{b\ H_s^2}{f(f/f_p)^4}\exp\left[\frac{-1.25}{(f/f_p)^4}\right]g^{\exp\left[\frac{-(f/f_p-1)^2}{2s^2}\right]} \qquad (16)$$

in which

$$b \cong \frac{0.0624}{0.230 + 0.033g - 0.185(1.9+g)^{-1}}$$

$$g = 3.3, \qquad s = \begin{cases} 0.07: & f \le f_p \\ 0.09: & f \ge f_p \end{cases}$$

A typical TMA spectrum is shown in figure 3. When combined with the spreading function (eq. 13), the directional wave spectrum is the result (eq. 12).

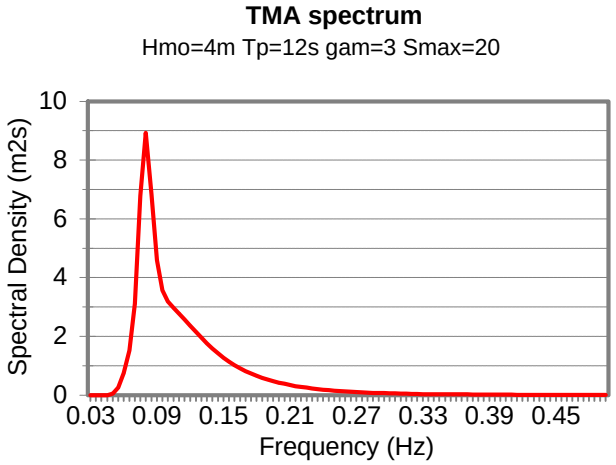

Figure 3. Example of the TMA frequency spectrum for waves in finite depths.

It should be noted that integration of the directional spectrum across all frequencies and directions by definition yields the total wave energy; i.e.,

$$m_0 = \int_0^{\infty} \int_{-p/2}^{p/2} S(f,q)\,dq\,df \qquad (17)$$

Because of the REF/DIF S directional limitation (50 degrees to either side of the x+ grid axis), a portion of the spectral energy calculated by eq. (17) may be lost depending upon the shape of the spreading function for the selected wave frequencies. In this study, eleven band-centered frequencies are selected in the range 0.035 to 0.5 Hz using a fixed bandwidth interval chosen so that the lowest and the highest frequencies span more than 96% of the total energy resulting from the first integration in eq. (17). Eleven directions relative to the grid are used, including one 0.0^0 direction coincident with the x+ grid axis and five directions at 10^0 intervals to either side.

Given the principal wave direction (θ_m) measured counterclockwise from the x+ grid axis, a representative wave amplitude is calculated for each *f,q* pair using eq. (12). These amplitudes are then entered as the first row of the computational grid and propagated forward (downwave) as REF/DIF S computes new solutions row by row. θ_m cannot be made very large or a significant fraction of the total wave energy will not be "gated" into the model domain.

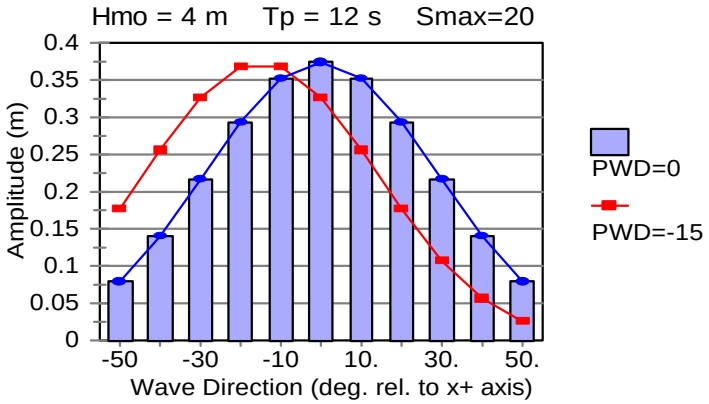

Figure 4. Graph showing wave amplitudes for 11 directions at *fp*=0.08 Hz before and after a change in principal wave direction (PWD).

Figure 4 illustrates this effect. If the principal wave direction, θ_m, is more than 15 degrees relative to the x+ grid axis, the model reference grid should be re-oriented to reduce θ_m accordingly.

Wave Climate Information

Spectral wave models such as REF/DIF S require detailed input information of the type discussed in the previous section. In order for the resulting model predictions to be representative, knowledge of the local wave climate is required. Directional wave observations for the nearshore region of Virginia Beach and Sandbridge do not exist; However, a 20-year simulated (hindcast) data set is available (Hubertz et al., 1993) and has been used as model input for the present study. Hubertz et al. (1993) provide a revision of an earlier data set created for the years 1956-1975, based on hindcast wind fields and using the latest Corps of Engineers wave hindcast model (WISWAVE 2.0). Information is given for 108 nearshore locations along the U.S. Atlantic coastline, stations 58 and 59 being applicable to the present study (Figure 5).

An examination of the WIS data for Atlantic Stations 58 and 59 shows that the largest hindcast Hmo heights are for waves arriving most frequently from 090^0 (east) and 045^0 (northeast). Tables 1 and 2 show the distributions for these directions at station 59. From Table 1 (045^0), the most extreme waves will have Hmo heights between 4 and 5 m with peak spectral

Table 1. WIS Hindcast Data 1956-1975, Atlantic Station 59.
Direction 022.5^0-067.5^0 (045^0), number of waves per category.

									Tp (sec)
Hmo(m)	4	6	8	**10**	**12**	14	16	18	20
0 - 1	1074	295	36	0	0	0	0	0	0
1 - 2	218	1054	92	1	0	0	0	0	0
2 - 3	0	80	236	12	0	0	0	0	0
3 - 4	0	0	27	42	16	0	0	0	0
4-5	0	0	0	**13**	**8**	0	0	0	0
5 - 6	0	0	0	0	0	0	0	0	0
6 - 7	0	0	0	0	0	0	0	0	0
7 - 8	0	0	0	0	0	0	0	0	0
8 - 9	0	0	0	0	0	0	0	0	0

Table 2. WIS Hindcast Data 1956-1975, Atlantic Station 59.
Direction 067.5^0-112.5^0 (090^0), number of waves per category.

					Tp (sec)				
Hmo(m)	4	6	8	10	**12**	**14**	**16**	18	20
0 - 1	908	1194	5060	5222	2267	540	112	23	2
1 - 2	81	1224	1256	1646	1226	418	28	0	0
2 - 3	0	50	386	405	211	115	24	2	0
3 - 4	0	0	29	131	134	50	2	2	0
4 - 5	0	0	0	16	58	21	0	1	0
5-6	0	0	0	0	**7**	**24**	**1**	0	0
6-7	0	0	0	0	0	**8**	0	0	0
7 - 8	0	0	0	0	0	0	0	0	0
8 - 9	0	0	0	0	0	0	0	0	0

periods between 10 and 12 seconds. From Table 2 (090^0) the most extreme waves will have Hmo heights between 5 and 7 m and peak spectral periods between 12 and 16 seconds. Values in this range were selected for REF/DIF S model simulations.

Model Reference Grid

The model reference grid used in this study is shown in figure 1. It extends 20 km in the shoreward (x+) direction and 24 km in the longshore (y+) direction. The origin of the grid (x=0, y=0) lies at the northernmost corner which has UTM coordinates 430988.48064, 4088916.01676 for UTM zone 18. The azimuth for the x+ grid axis is 255 degrees measured clockwise from true north. The reference grid cell size is 250 m x 250 m with interpolated depths provided at each grid intersection point. Depths in meters below mean lower low water (MLLW) were obtained at irregularly-spaced points from the NOAA/NOS bathymetric data base named GEODAS. Files searched in GEODAS were corrected to refer all horizontal reference coordinates to the North American Datum of 1983 (NAD 83). GEODAS-supplied depths were found to be sparse in a few specific locations such as the test firing range seaward of the Dam Neck Naval Facility.

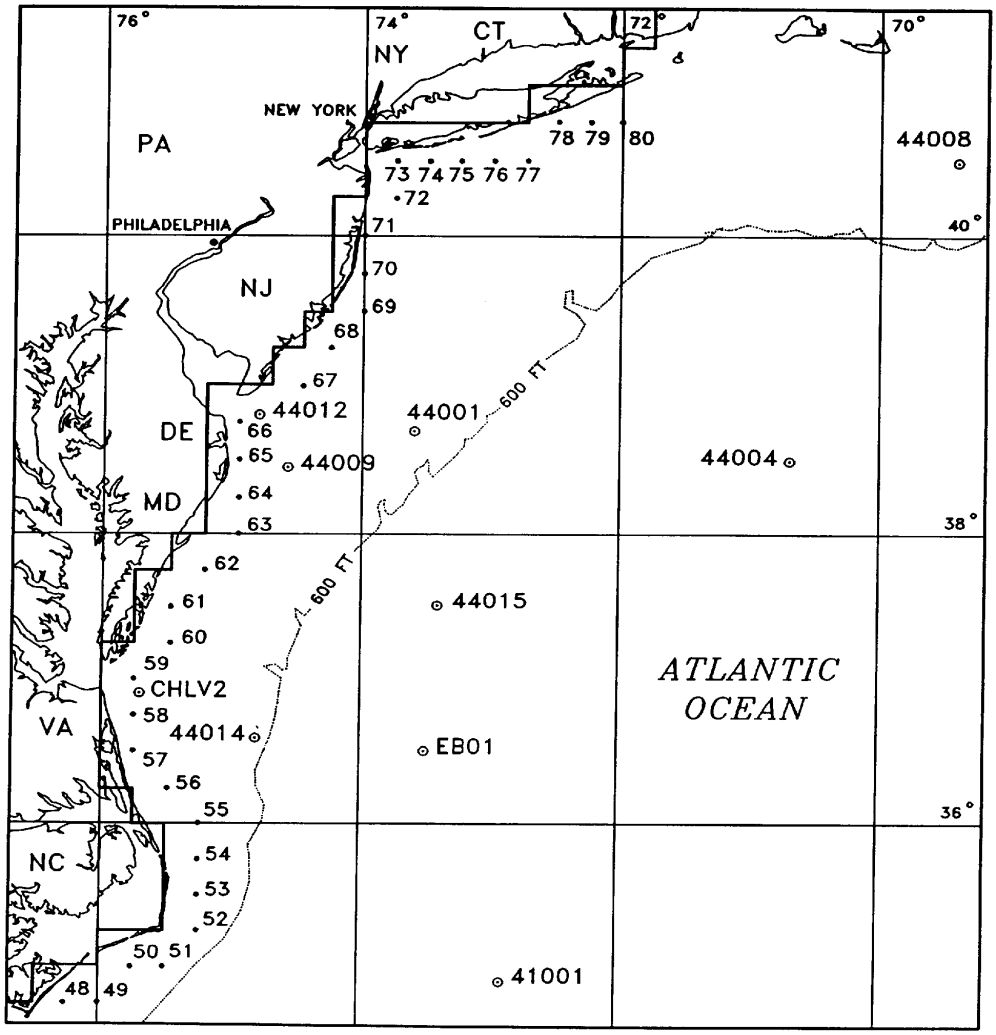

Figure 5. Map showing the location of WIS Atlantic Hindcast Wave Information Stations, U.S. Army Corps of Engineers. Other stations shown include NOAA observation buoys (e.g., 44001) and non-directional wave sensor at the Chesapeake Light Tower (CHLV2).

Supplemental soundings were obtained during a two-day, intensive hydrographic survey conducted by the NOAA ship FERREL in areas designated by the author. The resulting bathymetric grid for the Virginia Beach – Sandbridge coastal sector is shown in Appendix A, Plate 1.

While the reference grid horizontal spacing was fixed at 250 m x 250 m as noted above, the computational grid spacing actually used by REF/DIF S was made smaller through available

user options. Options were selected that subdivided y-axis spacings by four (to 62.5 m) and x-axis spacings by ten (to 25.0 m). The intervening depths were calculated by REF/DIF S at run-time using a linear, twisted surface routine.

Because of the present study focus on sand mining of the nearshore feature known as Sandbridge Shoal, an 8 km by 6 km subgrid was created to develop finer bathymetric detail in this region as shown in Appendix 1, Plate 2. Depths for the Sandbridge Shoal Subgrid were obtained at 25 m intervals in the x direction and at 62.5 m intervals in the y direction, thus matching the spacing of the computation grid discussed above. However, with a subgrid it is possible for the user to enter detailed depth information either to show high-density soundings representing the actual bottom or to develop hypothetical, fine-scale bathymetry (e.g., mounds or dredged areas) for test purposes. In displays such as the 3D mesh plot in Appendix A, Plate 2 (drawn using MATLAB Graphics), only every 4^{th} data point in the x-direction is shown.

Idealized Nearshore Bathymetry Model

Before propagating spectral waves across the actual bathymetry in the Virginia Beach - Sandbridge model domain, a series of test runs was conducted using a idealized approximation to that surface. The resulting model of the shoreface will be described before discussing the outcome of these runs.

A variation of Dean's equilibrium beach profile (Dean, 1977) was applied using the equation

$$h = A \cdot X^{m} \qquad (18)$$

where h = depth, X = distance from the shoreline in the seaward direction, and A, m are profile scale and shape parameters. Strictly speaking, eq. (18) is applicable only to the surf zone or a slight distance beyond in a region where bottom sediment is capable of being mobilized by wave action. In a theoretical derivation, Dean showed that m=2/3 results assuming uniform wave energy dissipation by spilling breakers across the surf zone and this value is the one generally

accepted by those who model natural beaches by this means. A similar assumption, however, yields m=0.4 and this value, along with A=0.39, results in the best fit in the least squares sense to the full profile crossing Sandbridge Shoal and continuing across the model domain to a maximum depth of about 20 m. The inshore part of this profile is shown in figure 6. The three-dimensional surface developed by extending the $h = 0.39 \times ^{0.4}$ profile uniformly in the y-direction is herein called the equilibrium shoreface surface (see Appendix A, Plate 3).

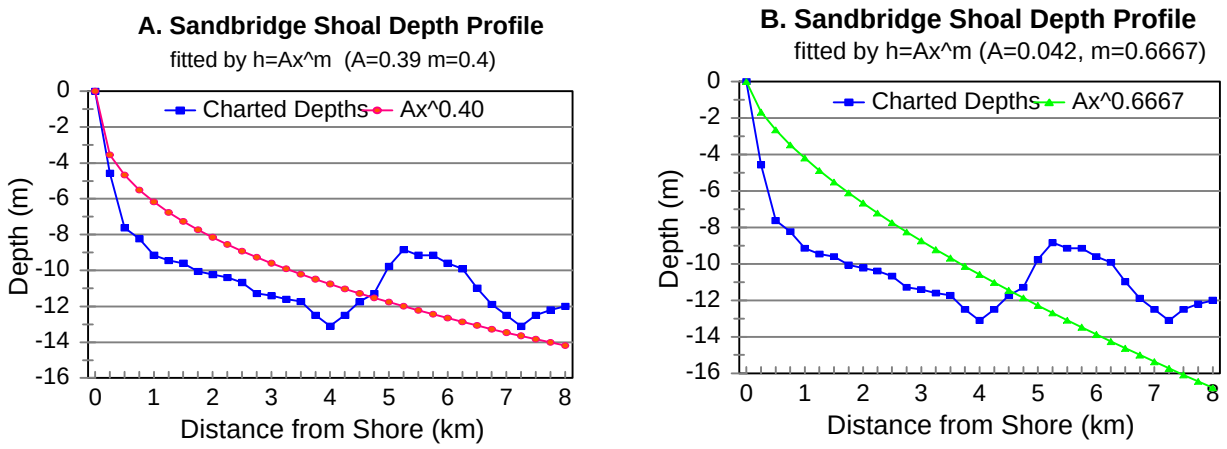

Figure 6. Equilibrium beach profile fitted to nearshore bottom in the Sandbridge subgrid using m=0.4 (A) and m=2/3 (B). m=2/3 (B) fails to match 20 m depth offshore.

From figure 6 (A), one of the simplest approximations to the natural bottom in the region of the Sandbridge Shoal subgrid is a surface developed using $h = 0.39 X^{0.4}$ with a mound rising 3 m above the surface to represent the shoal (Appendix A, Plate 3). The sides of the mound in Plate 3 have an approximately 1:10 slope with rounded corners. Using an idealized model of the upper shoreface at Sandbridge Shoal is by no means intended to replace the study of the actual bathymetry. It simply allows additional testing of a complex wave model to determine its response to changes in the basic elements of the bathymetry; i.e., the presence or absence of the shoal in its simplest configuration. The configuration is also one that can be easily replicated and tested by others who may have made improvements to REF/DIF S and perhaps other models that they wish to advance.

Equilibrium Shoreface Surface – Model Test Runs

1. General - Plate 1, Appendix B, illustrates the primary type of output that the REF/DEF S wave model is capable of producing; i.e., a surface contour plot of the Hmo wave heights distributed within the model domain. A moderate storm wave input was used (Hmo = 3 m, T_p = 11 s) as input for this run. Information on wave direction is more difficult to obtain. Although it combines a relatively large number of component waves of varying frequency and direction at each point on the computational grid, REF/DIF S does not generate directional spectra at these points and thus cannot produce vector plots of the spectral peak or principal wave direction. REF/DIF S does produce estimates of the radiation stress components S_{xx}, S_{xy}. and S_{yy}. These can be used to obtain information on gradients in radiation stress which define the driving force for longshore transport within the surf zone. Radiation stress gradients were not addressed in the present study.

2. Wave breaking – As previously noted, REF/DIF S uses the breaking model by Thorton and Guza (1983). Rather than handling wave breaking through an "on" "off" switch, eq. (11) is used continuously to determine a breaking coefficient that becomes very large at the onset of breaking, thus initiating rapid dissipation of wave energy as indicated in eq. (10). Plate 2A, Appendix B, shows the expected shore-parallel bands of diminishing wave height that begin a very rapid decay (breaking) within the final 300 m or so before reaching the shoreline. Plate 2B, Appendix B, shows a large area of affected wave heights down wave from the +3m mound placed 5m seaward of the shoreline. Wave heights increase by about 0.3 m at the lateral edges of the mound with smaller increases and decreases occurring in conically-spreading bands trailing the two edges. This perturbation on Hmo wave heights persists until within about 900 m of shore as the breaking band begins to develop. Within this band, longshore variations in Hmo effectively cease.

3. Principal Wave Direction - The Principal Wave Direction (PWD) in REF/DIF S is specified relative to the X+ reference grid axis. The latter has a heading of 255^0 measured clockwise from true north (000^0). The reciprocal of this heading is 075^0. Two test runs were made with a more

intense storm wave spectrum (Hmo = 4 m, T_p = 12s), varying the Principal Wave Direction by 15^0 to either side of the X axis. These directions conform to the WIS hindcast sectors (045^0 and 090^0) shown in Tables 1 and 2. Plates 3A and 3B, Appendix B, show the results of these runs using the test mound. A skewed distribution of wave heights appears to the right and left which are mirror images of one another or approximately so. This allows confidence in the assumption that the directional response is uniform; i.e., no lateral boundary effect even though the mound (and Sandbridge Shoal) is far from being centered within the reference grid.

4. Increase in offshore wave height - Increasing the height of the input wave offshore causes more pronounced longshore variations in Hmo wave height in the lee of the test mound, variations that extend closer to shore. This is clearly shown in Plates 2, 3, and 5 of Appendix B. In addition, the maximum offshore wave height tested (Hmo = 7 m, T_p = 15s) produced a strong, trident-shaped refraction-diffraction pattern in the lee of the rectangular mound (Plates 6A and 6B, Appendix B). As explained in the final section of the present report, this pattern was noted in other areas of the main reference grid when the actual bathymetry was used with the model.

5. Change in directional spreading parameter, S_{max} – Variations in S_{max} govern the degree of directional energy concentration as reflected by the narrowness of the directional spreading function about its peak value. The degree of directional spreading is known to affect both wave refraction and diffraction and is related to wave steepness (Goda, 1985). However, test runs using S_{max} = 10 (wind waves) and S_{max} = 20 (swell with short decay distance) for extreme storm waves (Hmo = 7m, Tp = 15s) show relatively small changes in wave height distributions (Plates 6A and 6B, Appendix B).

Model Runs with Existing and Locally Modified Bathymetry

1. **General -** Plate 1, Appendix C, shows what may be regarded as a typical example of moderately extreme storm wave propagation across the Virginia Beach- Sandbridge reference grid. The existing bathymetry (Plate 1, Appendix A) is more complex and reflects the fact that the actual Virginia Beach – Sandbridge shoreline is slightly concave seaward and the innermost depths are greater than zero (about 3m MLLW in the mid-section of the last row). The presence of two, trident-shaped, refraction-diffraction patterns ('crow's feet') can be seen, similar to but larger than, the patterns appearing down wave of the rectangular mound in the test runs. Plate 1 of Appendix C also shows that longshore variation in Hmo wave height is quite pronounced near the shoreline. Areas of lowest Hmo wave height appear to occur between the toes of the 'crow's feet'. The largest of these is situated immediately down wave of borrow area "A" at the crest of Sandbridge Shoals.

2. **Depth of Dredging, Borrow Area "A" –** Dredging has been done in borrow area "A" to depths of approximately -1 to –2 m, with –3 m occurring in some areas. For the purpose of wave model analysis to determine the possible impact of dredging, it was assumed that borrow area "A" was either un-dredged (condition 1) or dredged uniformly to a depth of –3 m (condition 2). It is estimated that the total yield for condition 2 would be 8.2 million cubic yards (6.3 million cubic meters). A comparison of plates 2A and 2B, Appendix C, suggests that the effect of this amount dredging would be to increase Hmo wave heights in limited areas offshore while creating a wider zone of low wave heights approaching the surf zone off Sandbridge Beach.

3. **Extreme Wave Conditions -** Extreme waves (Hmo = 5 to 7 m, T_p = 12 to 15 s) cause much larger waves to reach farther into the nearshore zone, particularly at the south end of the reference grid near Sandbridge Shoals and Sandbridge Beach (Plates 3 and 5, Appendix C). The effect of dredging borrow area "A" still appears to be one of lessening, not increasing, Hmo wave heights in the down wave shadow-zone approaching the surf zone. The decrease, however, is not large; i.e., less than 0.5 m in most places.

4. **Change in directional spreading parameter, S_{max} -** As with the test runs presented in Appendix B, using different values of S_{max} causes only a slight change in the distribution of Hmo wave heights as can be seen in Plates 7A and 7B, Appendix C. The change that results is much less than the change that occurs due to dredging (Plates 6A and 6B, Appendix C).

Summary and Conclusions

This investigation has shown that a spectral wave model, such as REF/DIF S, offers considerably more insight into the behavior of random wave fields in nature than is possible to achieve using a monochromatic wave model. Although intuitive guidance such as the depiction of wave refraction by means of converging or diverging wave rays is not possible with a spectral model, the latter does provide a critically important statistical basis for describing wave heights locally and throughout the model domain. The key parameter in that instance is the zero-moment wave height or its equivalent, the significant wave height.

In addition to its spectral wave features, REF/DIF S has another feature that is extremely useful, namely the subgrid. One can divide the rectangular reference grid into smaller cells within any selected sub-region to define a subgrid. The finer resolution of the subgrid is used only where needed to develop small-scale bottom features in detail while simultaneously allowing wave transformation to be studied over a much broader region. In this study, bottom features with length scales on the order of tens of meters were investigated within a 6 x 8 km subgrid using a 62.5 x 25 m cell size. The subgrid in turn was placed within a 20 x 24 km reference grid with 250 x 250 m cell size. In this way, deep water waves were transmitted from offshore sites, where spectral wave information was available, to the local site of immediate

concern, a region beginning at Sandbridge Shoal and extending landward to the surf zone in front of Sandbridge Beach.

The results of the wave modeling described in this report indicates that full development of a dredging site at Sandbridge Shoal, known as borrow area “A”, will cause slight but clearly perceptible changes in Hmo wave heights on the order of 0.5 m with higher differences in isolated regions near the site. In general, the effect of dredging will be to reduce wave heights slightly in a cone-shaped region between borrow area “A” and the surf zone. Although the model predicts uniform and rapid wave decay (wave breaking) in the surf zone, there are clear indications of significant longshore variations in Hmo wave height of a cyclical nature that will likely contribute to the forcing that enables two-dimensional circulation (rip currents) within the surf zone. More research is needed in this area, particularly with regard to longshore variations in wave height and local gradients in radiation stress.

References

Dalrymple, R.A. and J.T. Kirby, 1991. "*REF/DIF 1 version 2.3, Documentation Manual*", Report No. CACR 91-2, Center for Applied Coastal Research, Dept. of Civil Engineering, Univ. of Delaware, Newark, 19p.

Dean, R.G., 1977. "*Equilibrium beach profiles: U.S. Atlantic and Gulf coasts*", Ocean Eng. Tech. Rep. No. 12, University of Delaware, Newark.

Goda, Y., 1985. *Random seas and design of maritime structures,* University of Tokyo Press, 309 p., Appendix.

Hasselmann, K., T. Barnett, E. Bouws, H. Carlson, D. Cartwright, K. enke, J. Ewing, H. Gienapp, D. Hasselmann, P. Kruseman, A. Meerburgh, P. Muller, D. Olbers, K. Richter, W. Sell and H. Walden, 1973. "*Measurement of wind-wave growth and swell decay during the Joint North Sea Wave Project (JONSWAP*), Deutsches Hydrographisches Zeitschrift Reihe A (8^0), No. 12.

Hubertz, J.M., R.M. Brooks, W.A. Brandon, B.A. Tracy, 1993. "*Wave information studies of U.S. coastlines: Hindcast wave information for the U.S. Atlantic coast*", WIS Report 30, U.S. Army Corps of Engineers, Waterways Experiment Station, Vicksburg, MS., 20p., three appendices.

Hughes, S.A., 1984. "*The TMA shallow-water spectrum, description and applications*", Tech. Rep. CERC-84-7, U.S. Army Waterways Experiment Station, 39 p., appendix.

Kirby, J.T., 1986. "Higher-order approximations in in the parabolic equation method for water waves", *J. Geophys. Res.,* **91**:933-952.

Kirby, J.T. and R.A. Dalrymple, 1986. "An approximation model for nonlinear dispersion in monochromatic wave propagation models", *Coast. Eng*., **9**: 545-561.

Kirby, J.T., and H.T. Ozkan, 1992. "*Combined refraction/diffraction model for spectral wave conditions: documentation and user's manual*", Report No. CACR-92-06, Center for Applied Coastal Research, Dept. of Civil Engineering, Univ. of Delaware, Newark, 102p.

Thorton, E.B. and R.T. Guza, 1983. "Transformation of wave height distribution", *J. Geophys. Res*., **88**:5925-5938.

APPENDIX A

REF/DIF S WAVE MODEL BATHYMETRY

Bathymetry developed for REF/DIF S and the Virginia Beach – Sandbridge reference grid consists of a matrix of water depths corresponding to the array of regularly-spaced grid intersection points covering the model domain.

Actual water depths relative to mean lower low water were obtained from NOAA hydrographic surveys. In addition, a hypothetical Equilibrium Shoreface Surface (ESS) was developed for testing purposes using $h(x,y) = A \times^{m}$ with A=0.39, m=0.4. In some of these tests, an underwater mound was placed on the ESS at a distance of 5km from shore.

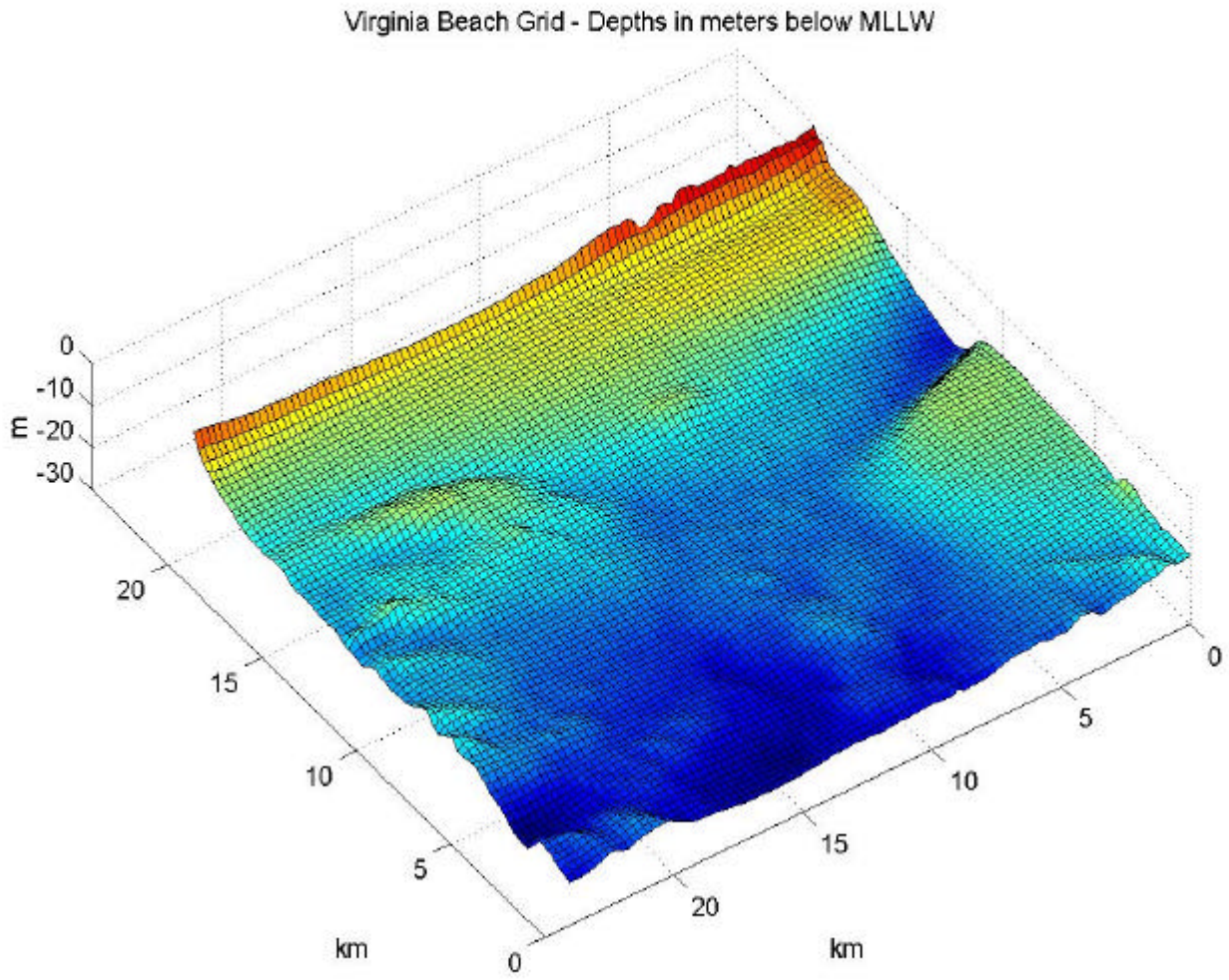

Plate 1. Bathymetry for the Virginia Beach – Sandbridge model reference grid.

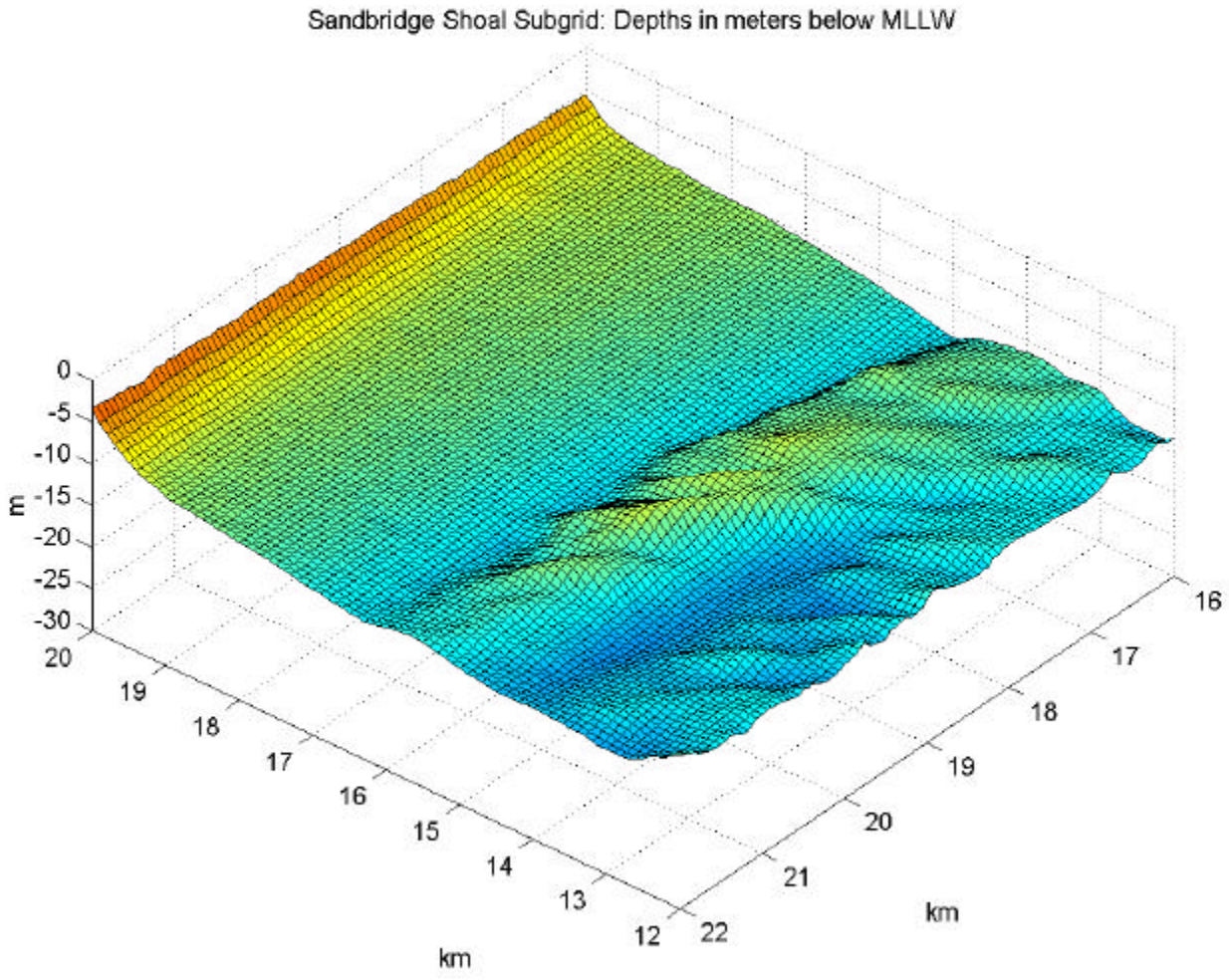

Plate 2. Location and bathymetry of Sandbridge Shoals subgrid

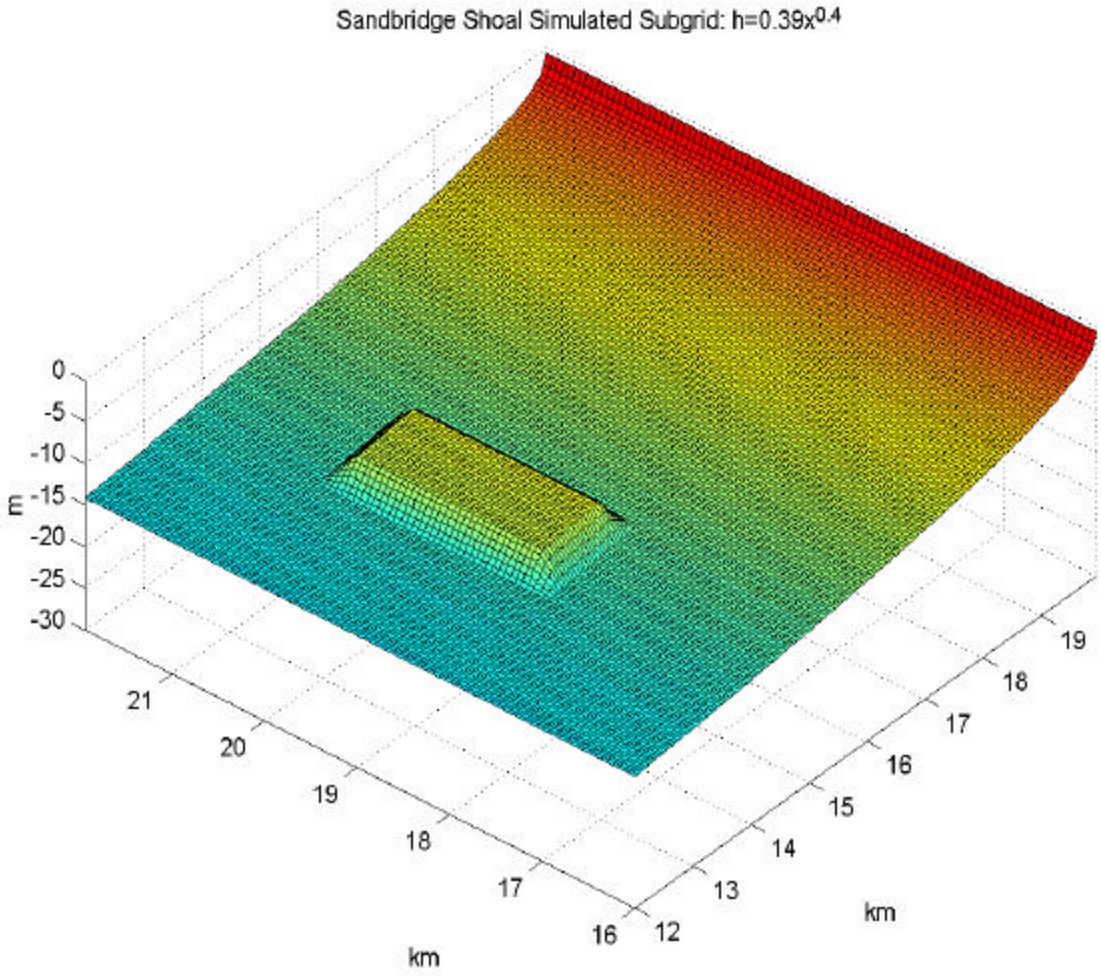

Plate 3. Equilibrium Shoreface Surface, Sandbridge Shoal subgrid.

APPENDIX B

REF/DIF S WAVE MODEL TEST RUNS

Test runs made using a hypothetical Equilibrium Shoreface Surface, $h(x,y) = A x^{m}$ with A=0.39, m=0.4 for the Virginia Beach – Sandbridge reference grid. Tests include selected runs with an underwater mound placed on the ESS at a distance of 5km from shore.

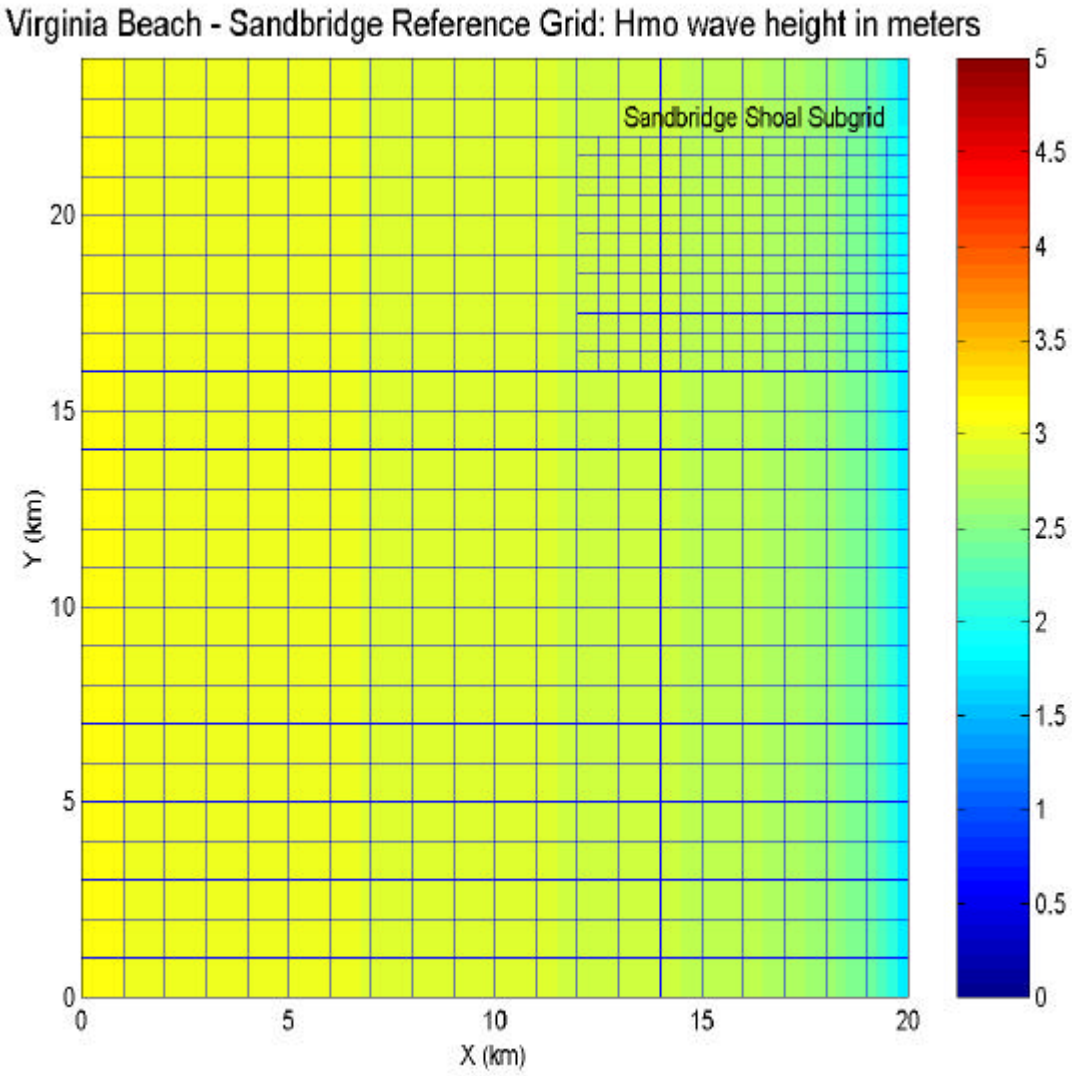

Plate 1. Model reference grid and color display of Hmo wave heights.
Model run 01: Hmo=3m, Tp=11s, Smax=10, PWD=0.

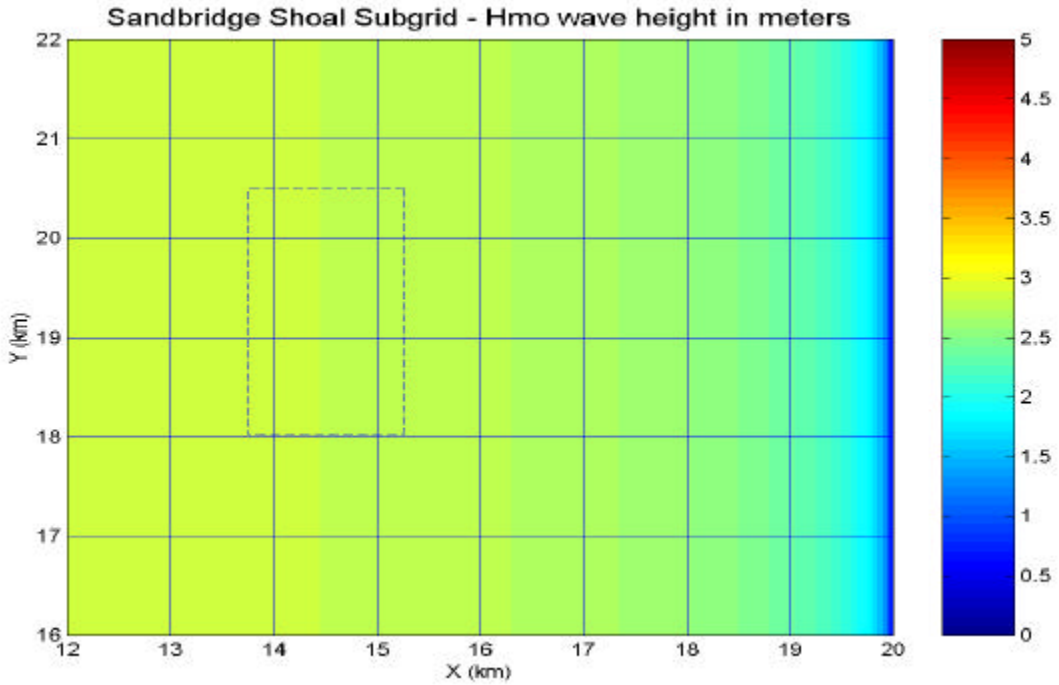

Plate 2A. Model run 01: Hmo=3m, Tp=11s, Smax=10, PWD=0
Condition: Test mound (dashed line) absent

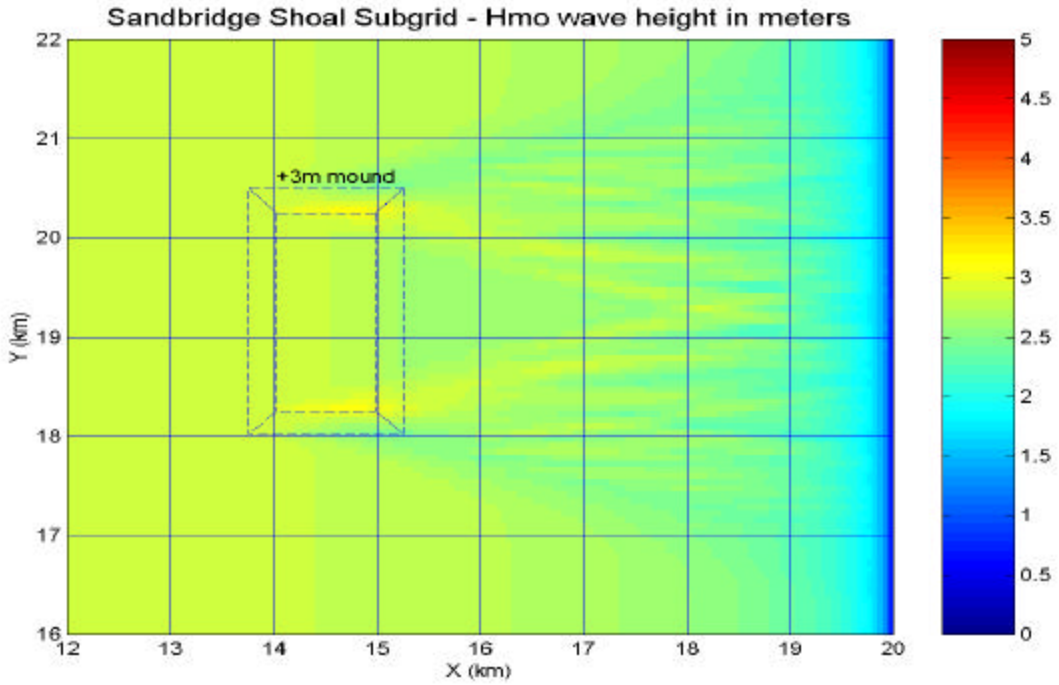

Plate 2B. Model run 02: Hmo=3m, Tp=11s, Smax=10, PWD=0
Condition: +3m test mound (dashed line) present

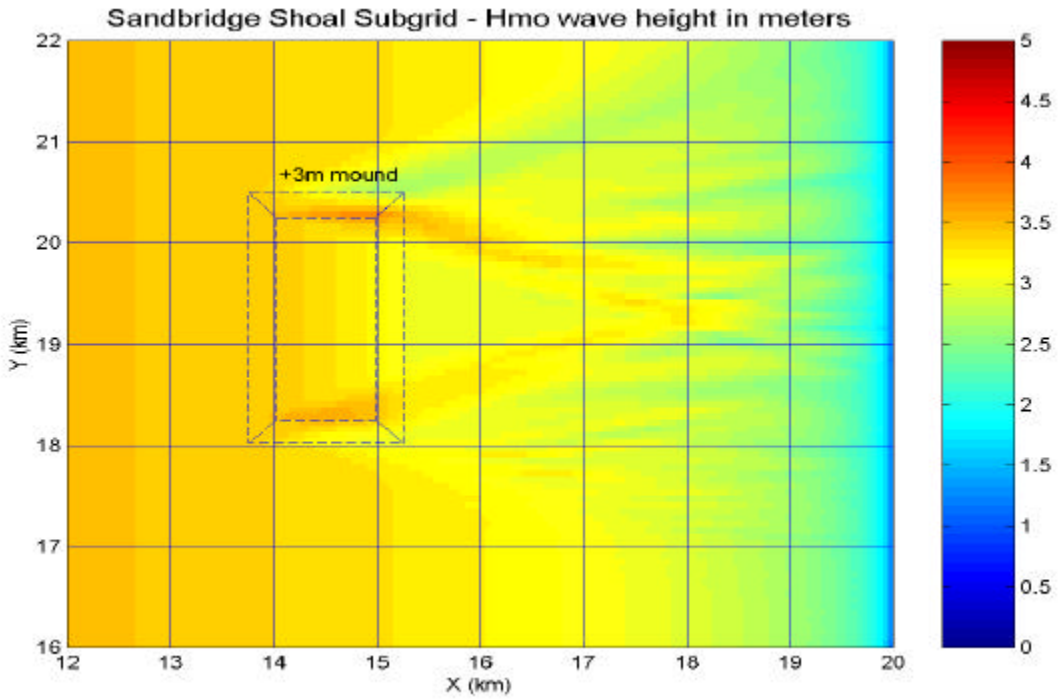

Plate 3A. Model run 03: Hmo=4m, Tp=12s, Smax=20, PWD=15
Condition: +3m test mound (dashed line) present

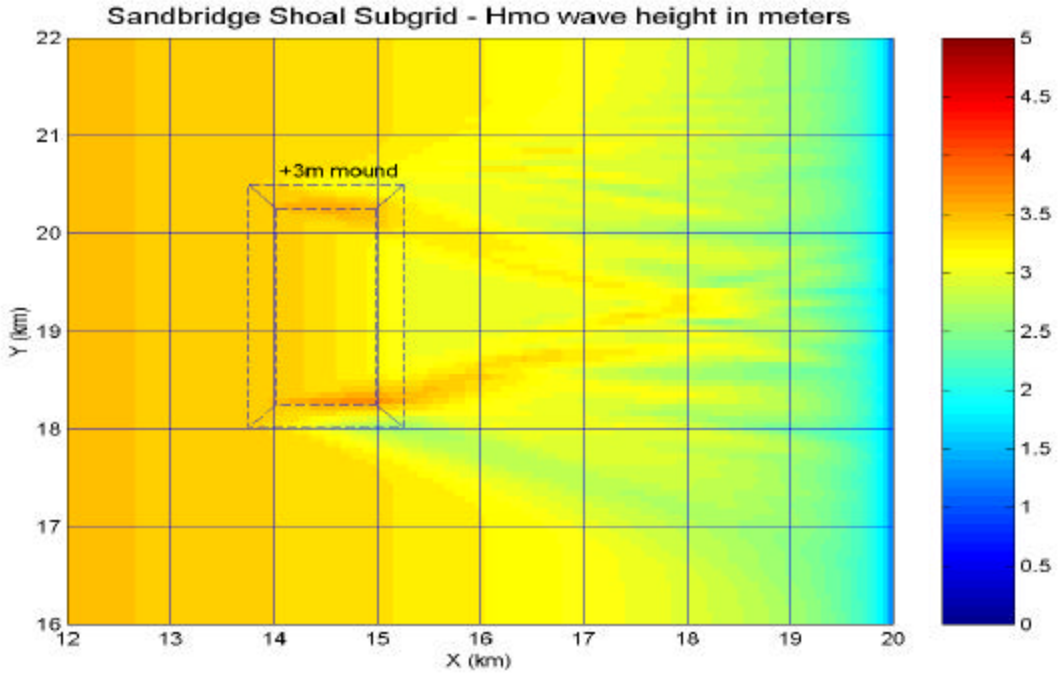

Plate 3B. Model run 04: Hmo=4m, Tp=12s, Smax=20, PWD= -15
Condition: +3m test mound (dashed line) present

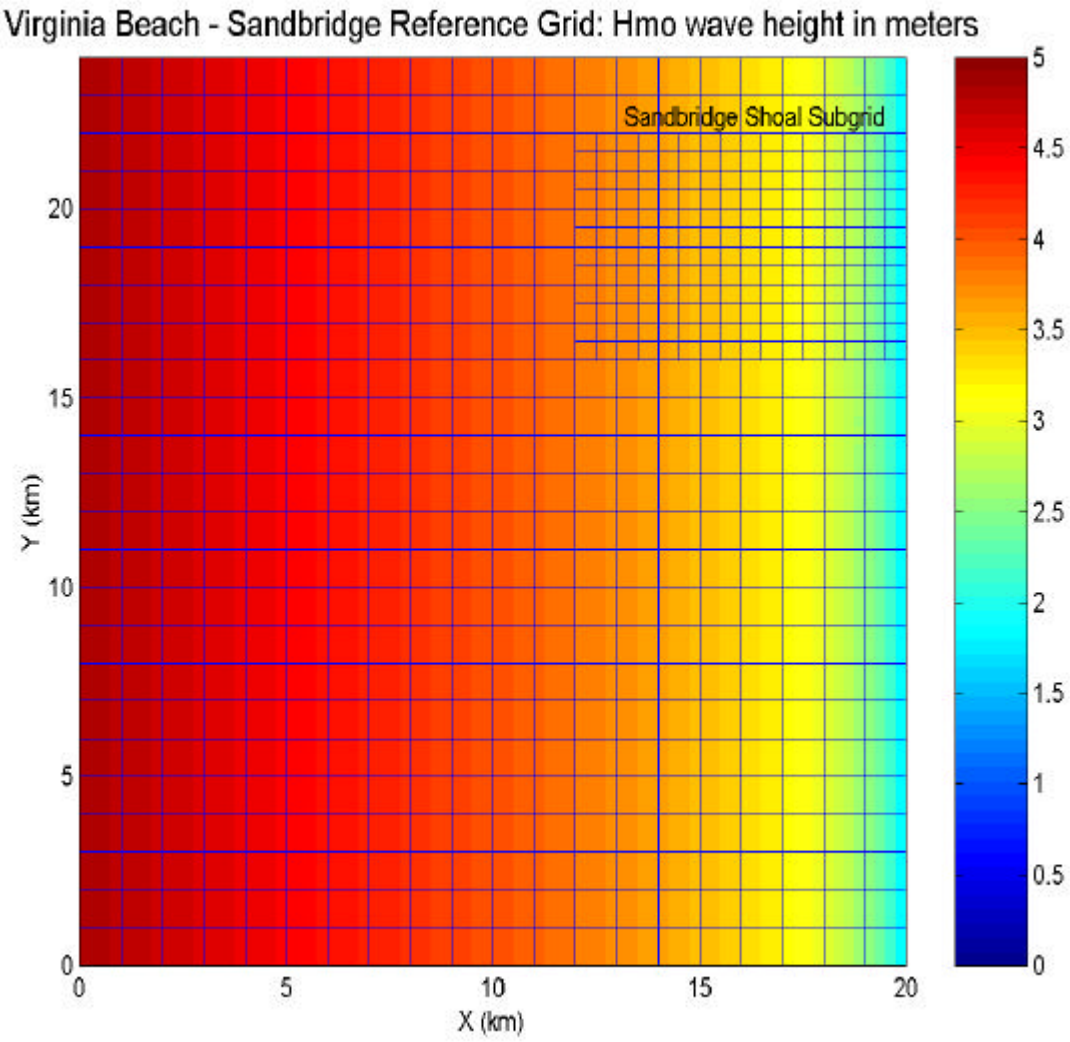

Plate 4. Reference grid and color display of Hmo wave heights.
Model run 05: Hmo=5m, Tp=12s, Smax=10, PWD=0.

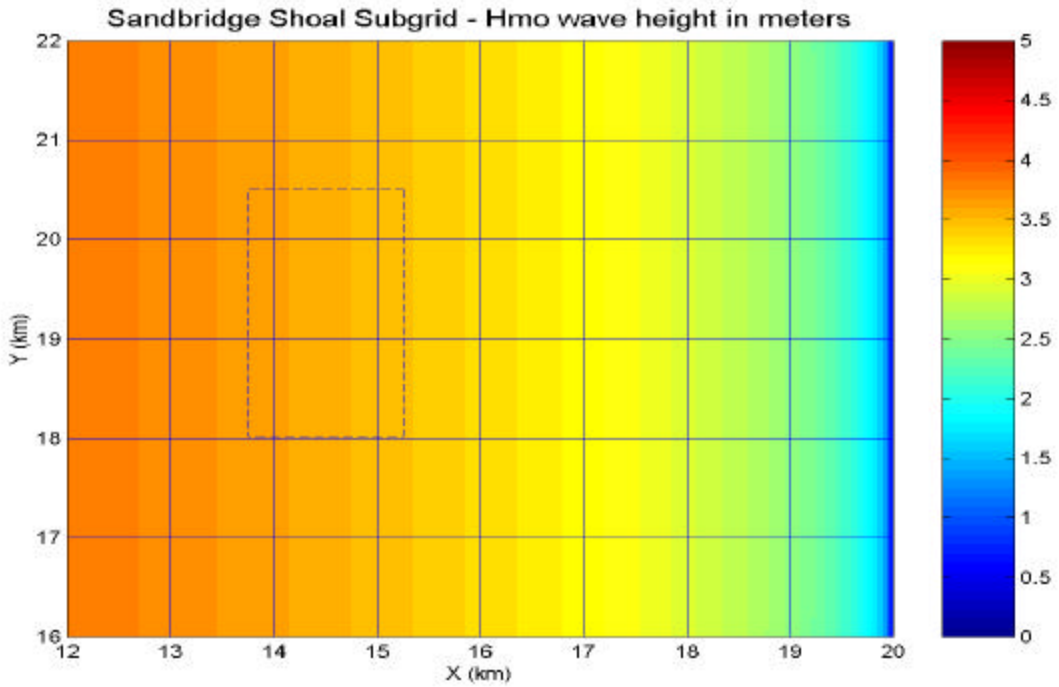

Plate 5A. Model run 05: Hmo=5m, Tp=12s, Smax=10, PWD= 0
Condition: test mound (dashed line) absent

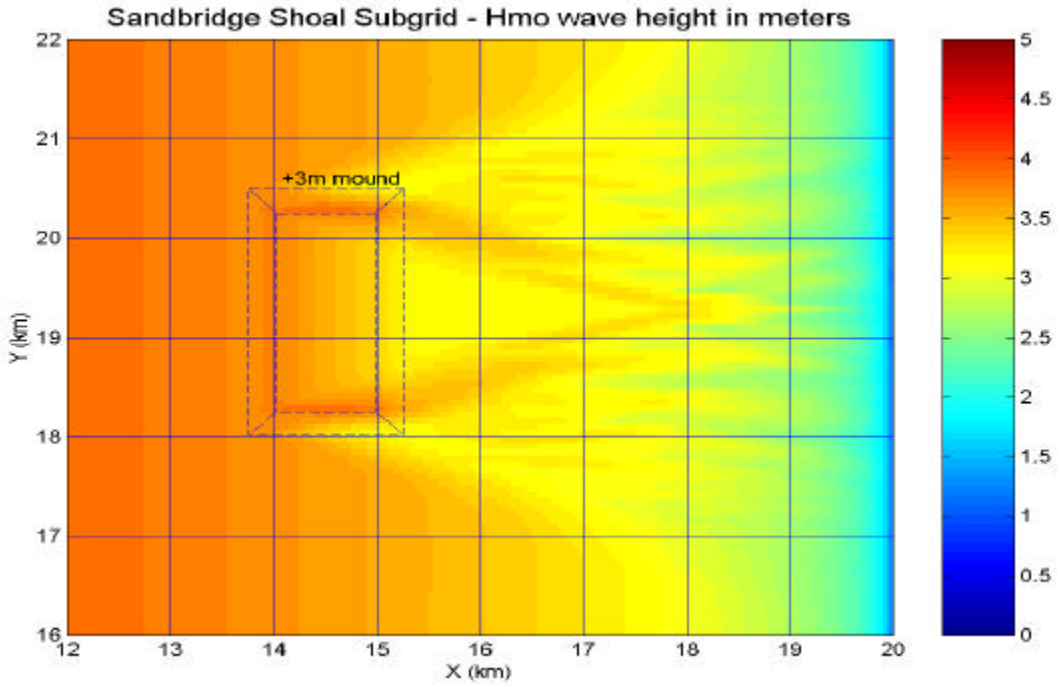

Plate 5B. Model run 06: Hmo=5m, Tp=12s, Smax=10, PWD= 0
Condition: +3m test mound (dashed line) present

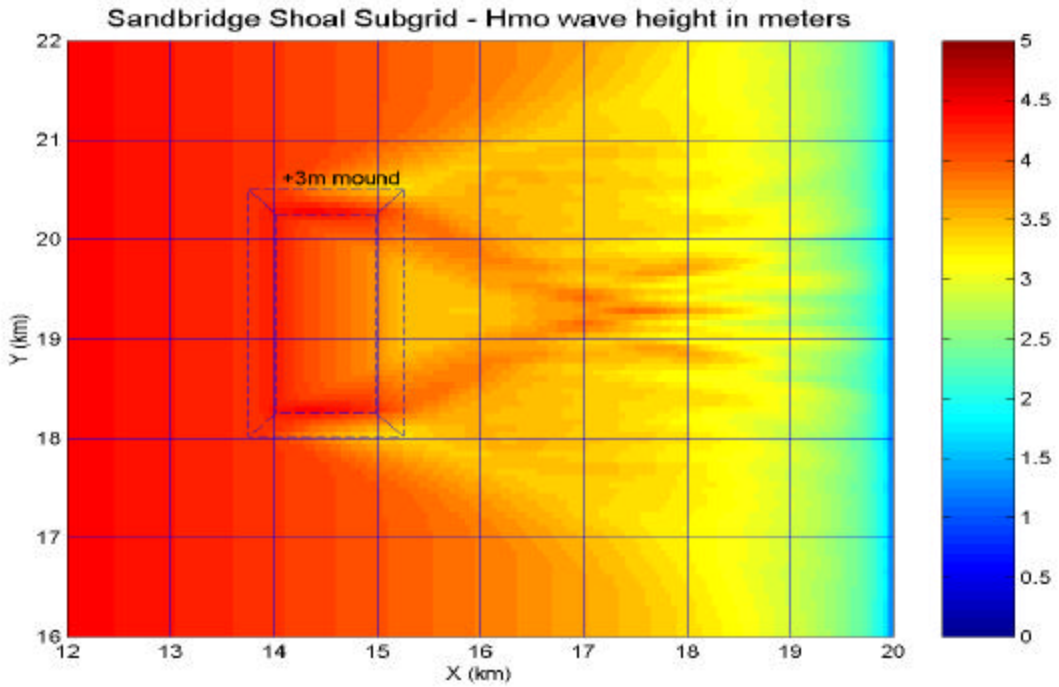

Plate 6A. Model run 07: Hmo=7m, Tp=15s, Smax=10, PWD= 0
Condition: +3m test mound (dashed line) present

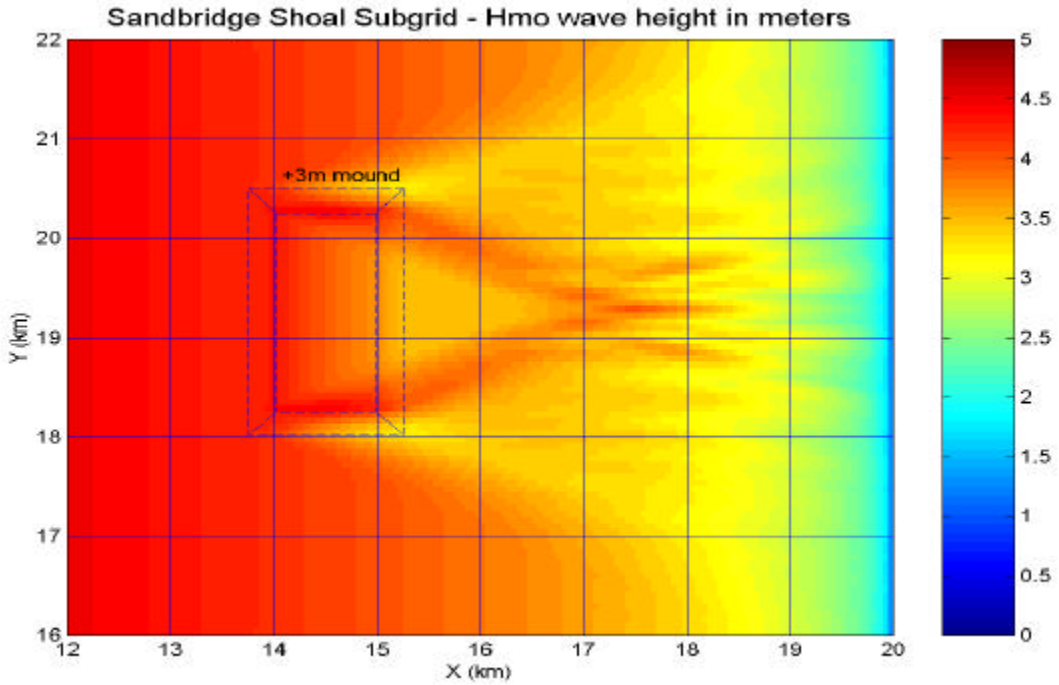

Plate 6B. Model run 08: Hmo=7m, Tp=15s, Smax=20, PWD= 0
Condition: +3m test mound (dashed line) present

APPENDIX C

REF/DIF S WAVE MODEL SITE RUNS

Model runs made using local bathymetry for the Virginia Beach – Sandbridge reference grid. Selected runs made to show effects of dredging borrow area “A” to a depth of –3 m.

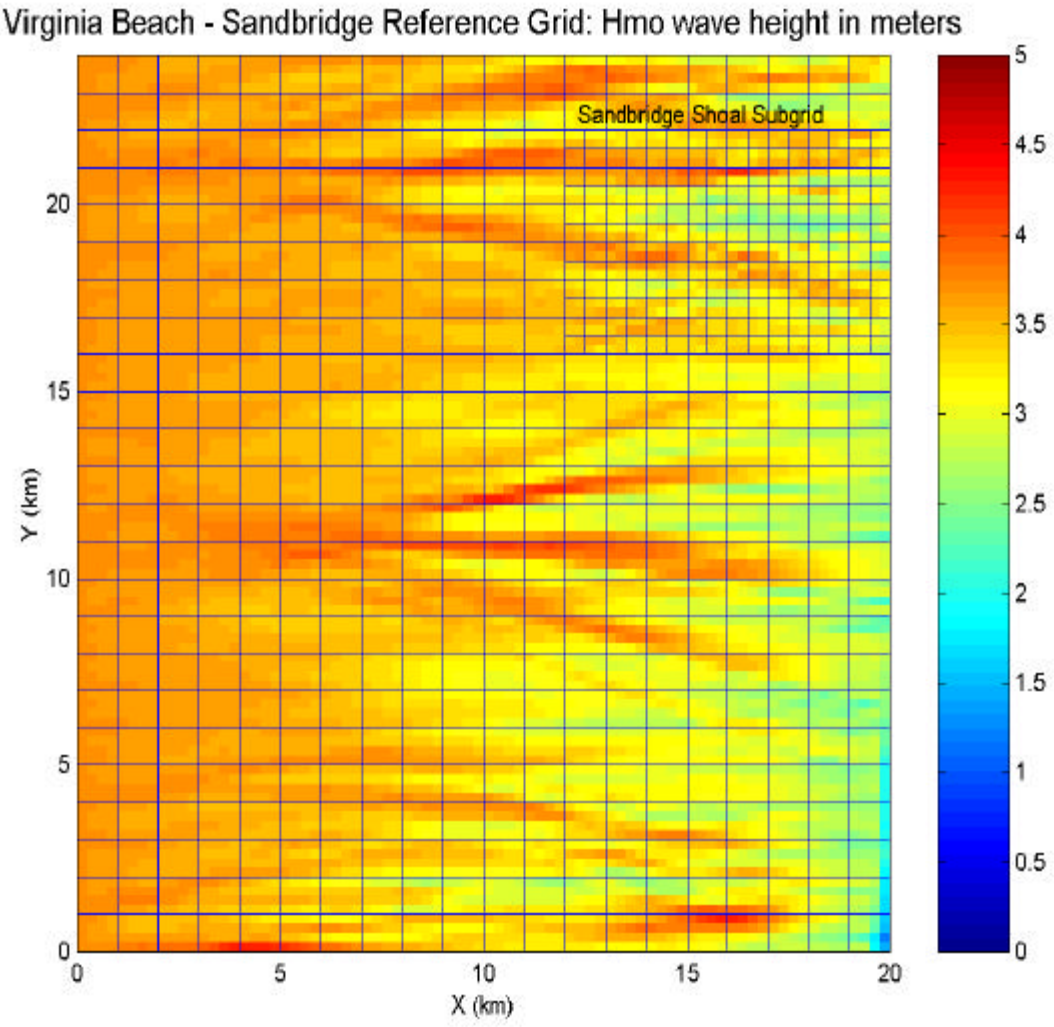

Plate 1. Model reference grid and color display of Hmo wave heights.
Model run 16: Hmo=4m, Tp=12s, Smax=10, PWD=0.

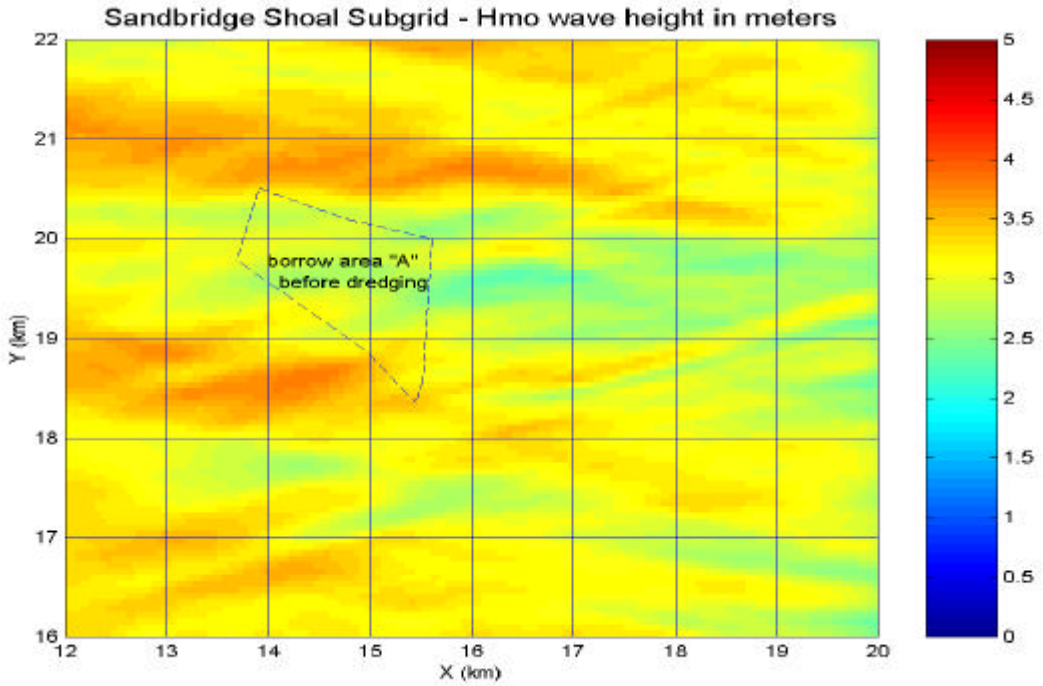

Plate 2A. Model run 17: Hmo=4m, Tp=12s, Smax=10, PWD= 0
Condition: Area “A” (dashed line) before dredging.

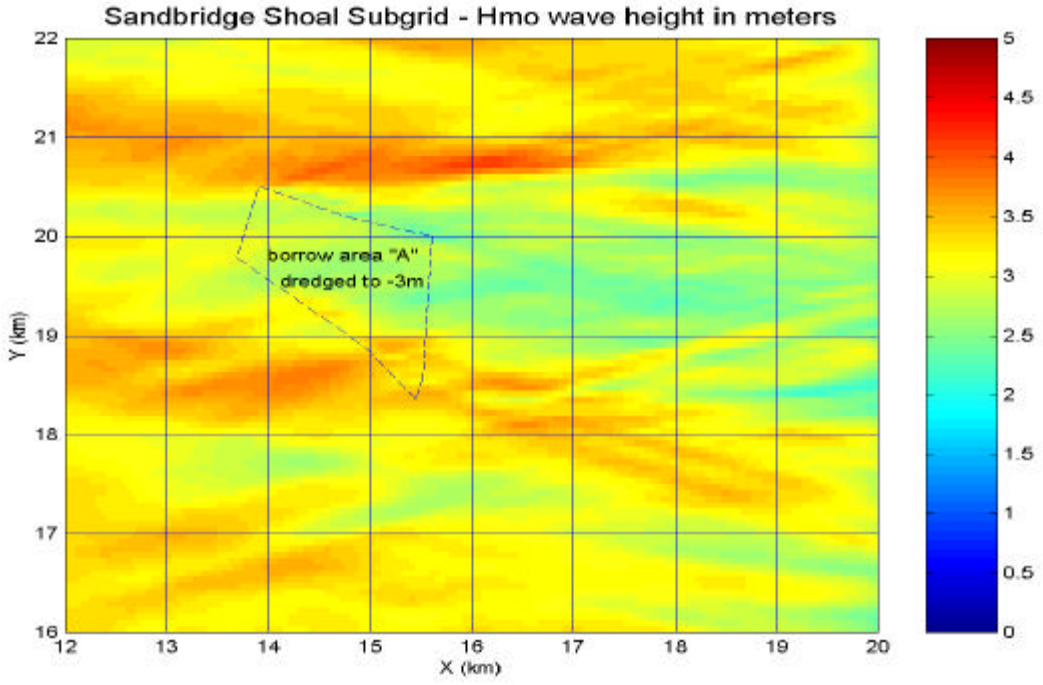

Plate 2B. Model run 16: Hmo=4m, Tp=12s, Smax=10, PWD= 0
Condition: Area “A” (dashed line) dredged to –3m.

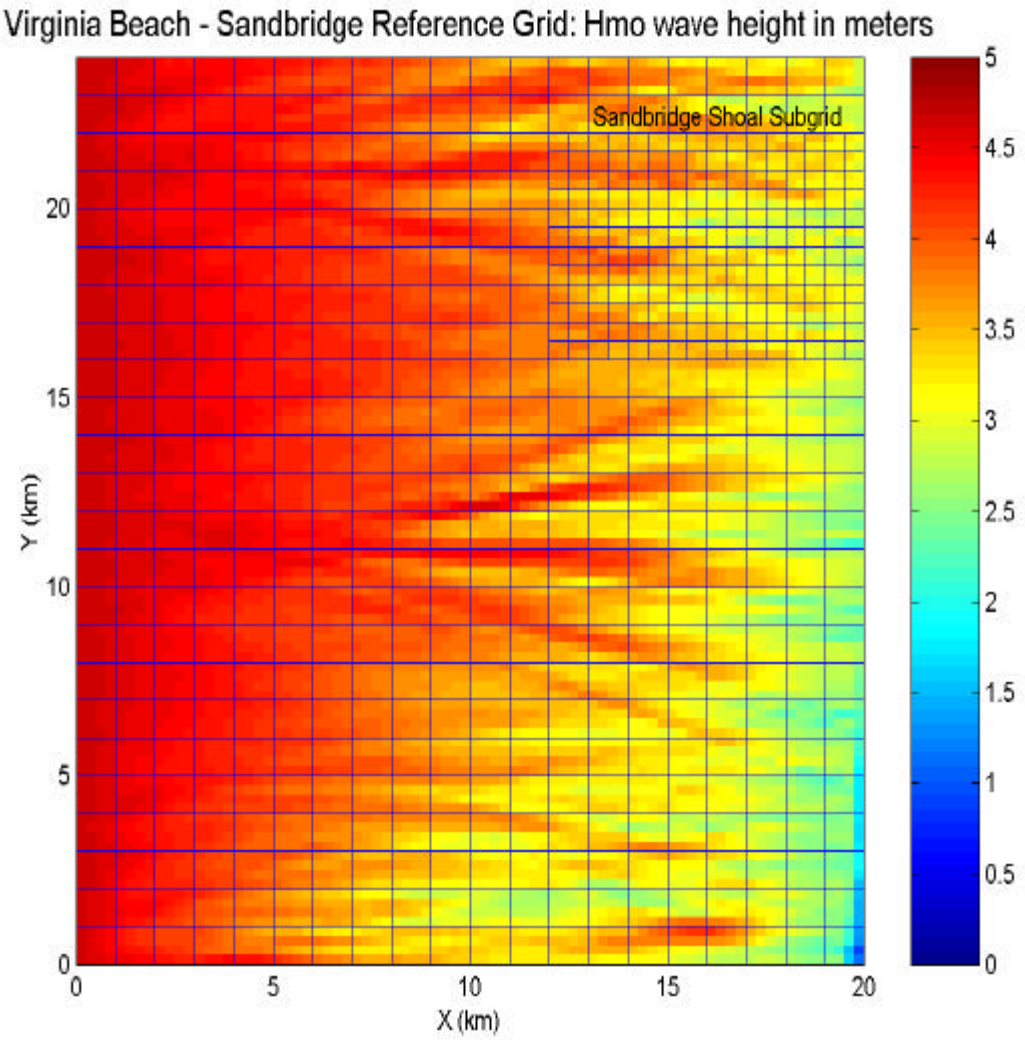

Plate 3. Model reference grid and color display of Hmo wave heights. Model run 18: Hmo=5m, Tp=12s, Smax=20, PWD=0.

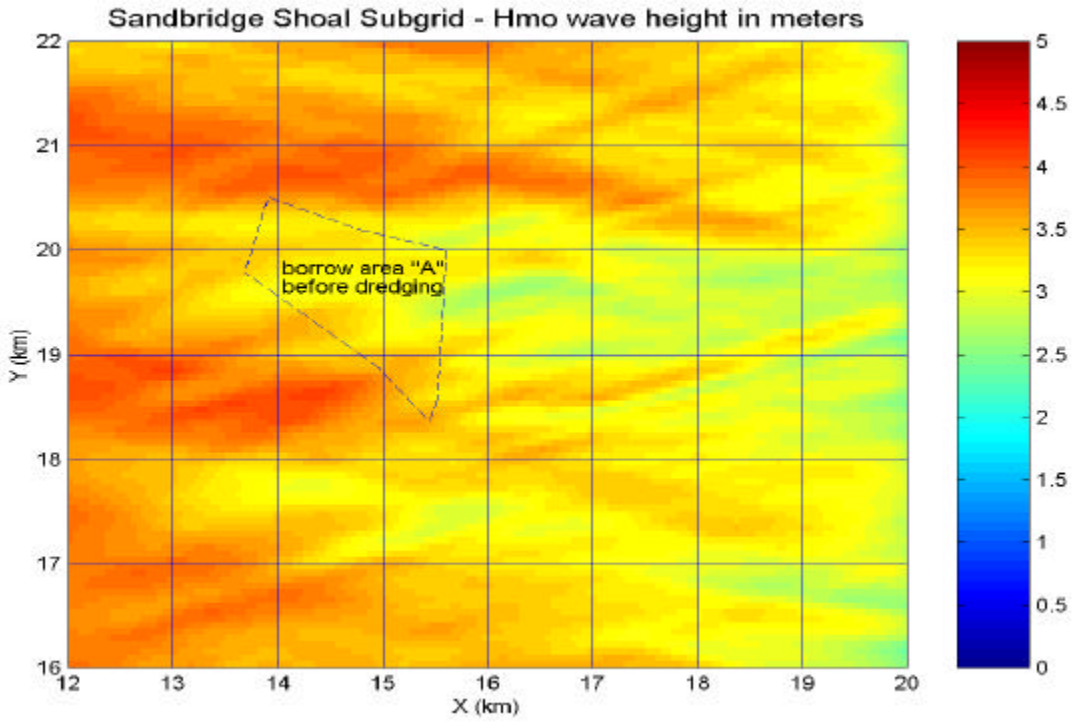

Plate 4A. Model run 18: Hmo=5m, Tp=12s, Smax=20, PWD= 0
Condition: Area "A" (dashed line) before dredging.

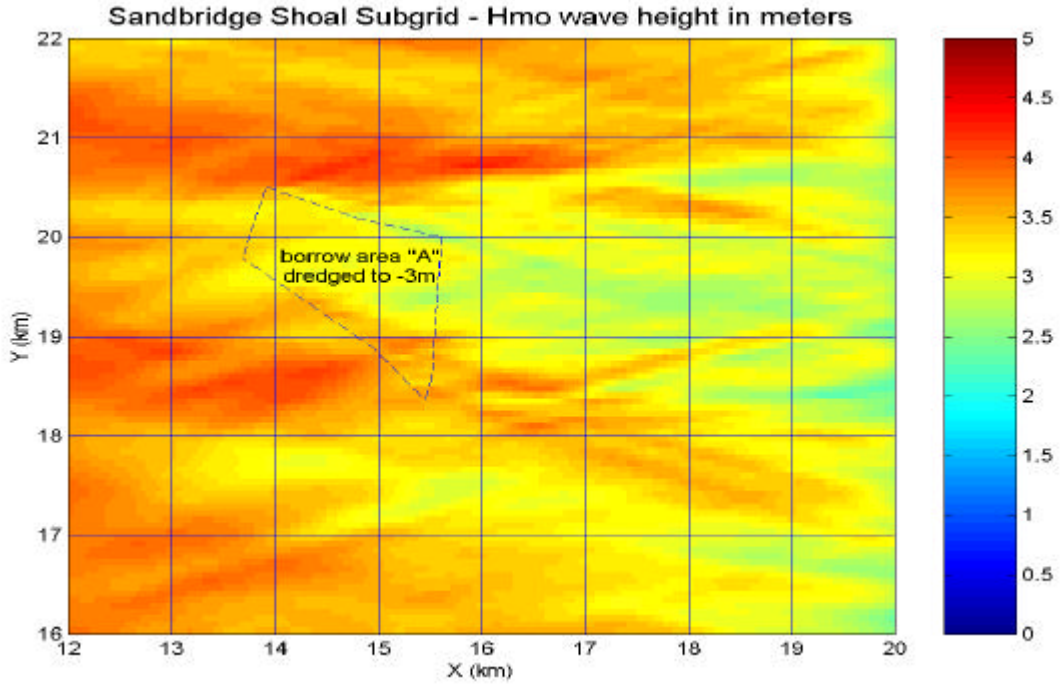

Plate 4B. Model run 19: Hmo=5m, Tp=12s, Smax=20, PWD= 0
Condition: Area "A" (dashed line) dredged to –3m.

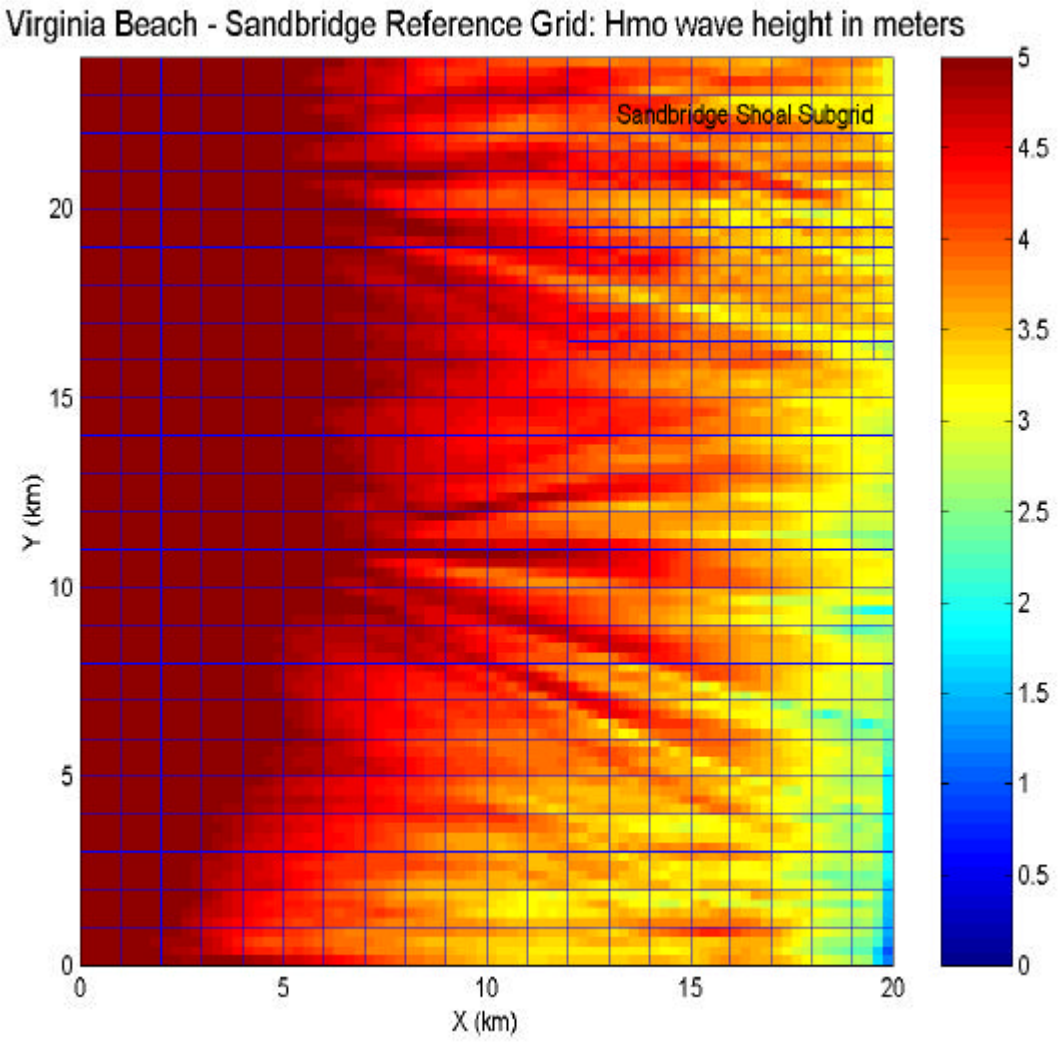

Plate 5. Model reference grid and color display of Hmo wave heights. Model run 20: Hmo=7m, Tp=15s, Smax=20, PWD= -15.

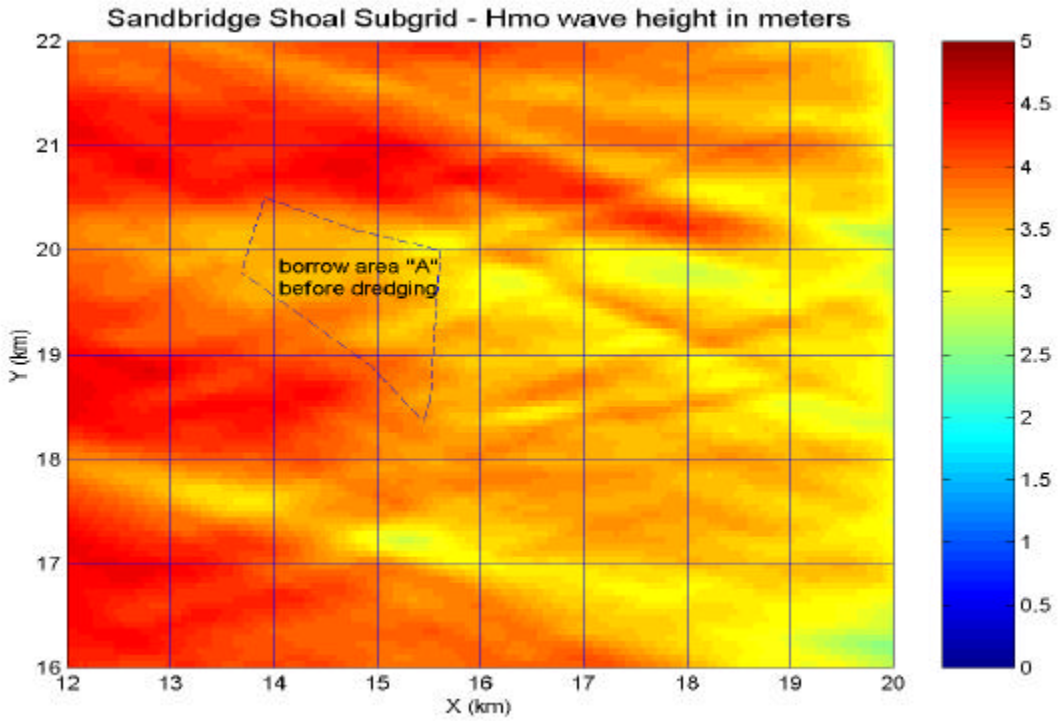

Plate 6A. Model run 20: Hmo=7m, Tp=15s, Smax=20, PWD= -15
Condition: Area “A” (dashed line) before dredging.

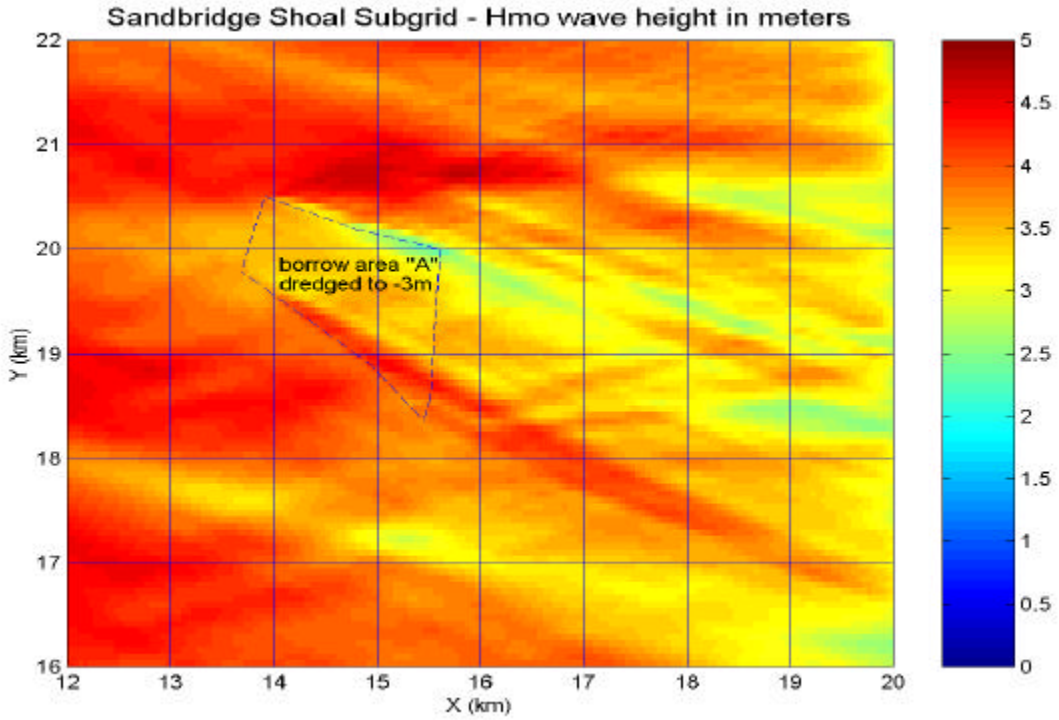

Plate 6B. Model run 21: Hmo=7m, Tp=15s, Smax=20, PWD= -15.
Condition: Area “A” (dashed line) dredged to –3m.

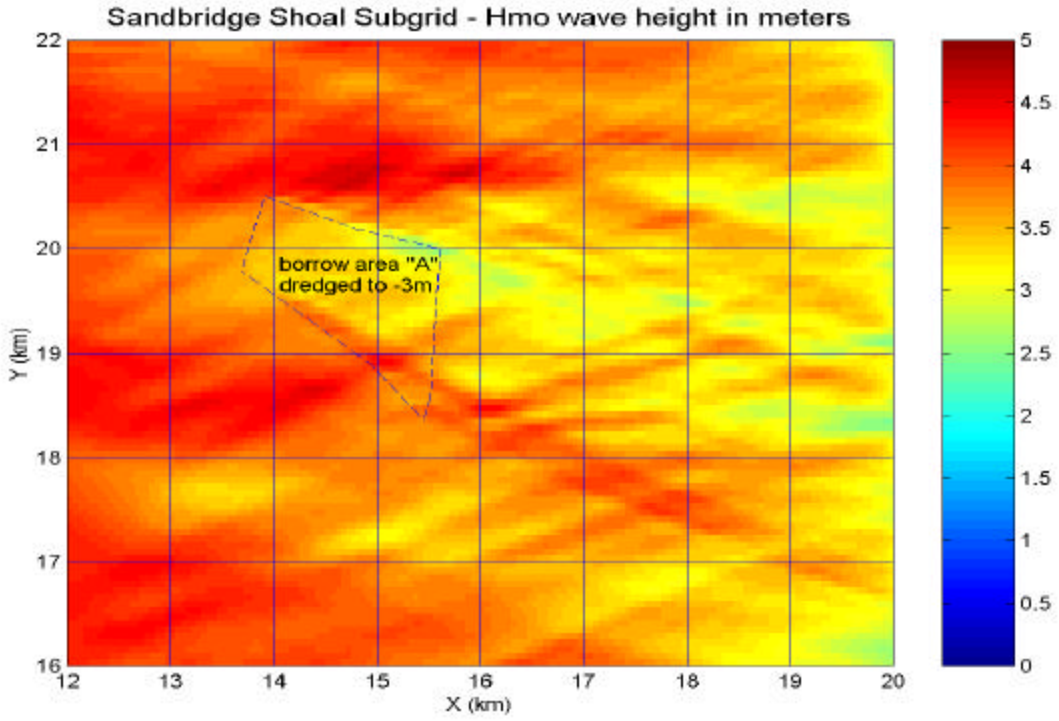

Plate 7A. Model run 22: Hmo=7m, Tp=15s, Smax=10, PWD=0.

Condition: Area “A” (dashed line) dredged to –3m.

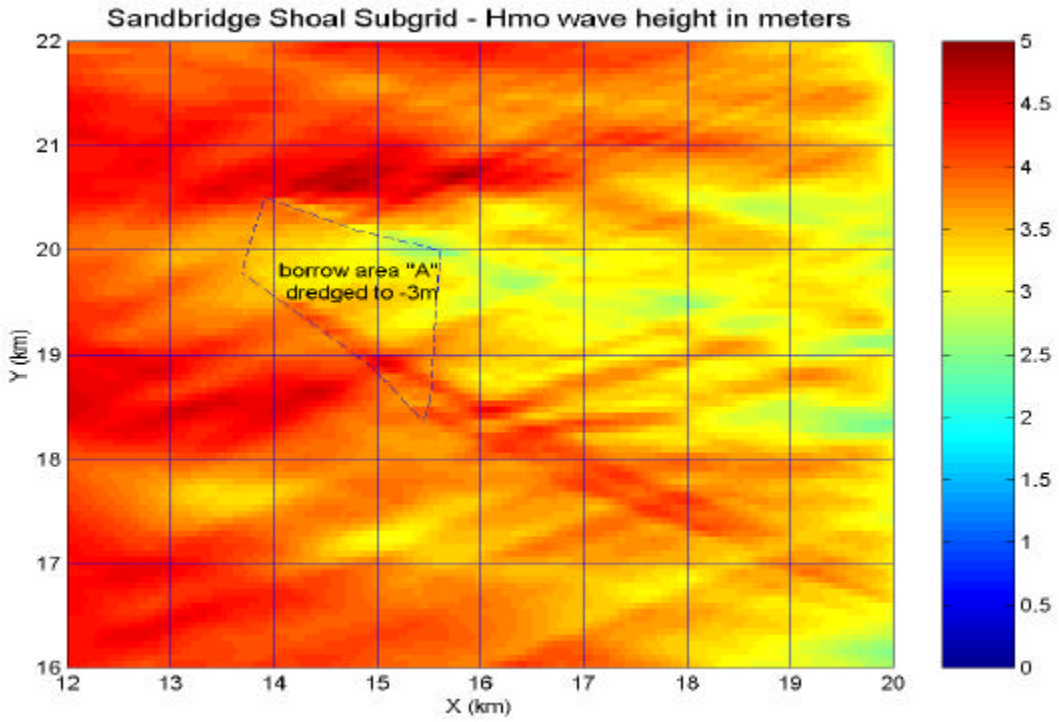

Plate 7B. Model run 23: Hmo=7m, Tp=15s, Smax=20, PWD=0.
Condition: Area “A” (dashed line) dredged to –3m.